University of Alberta

Self Consistent Modification To The Electron Density Of States Due To Electron-Phonon Coupling In Metals

by

Fatih Doğan

A thesis submitted to the Faculty of Graduate Studies and Research in partial fulfillment of the requirements for the degree of Master of Science.

Department of Physics

Edmonton, Alberta

Spring 2003

National Library of Canada
Acquisitions and Bibliographic Services
395 Wellington Street
Ottawa ON K1A 0N4
Canada

Bibliothèque nationale du Canada
Acquisitions et services bibliographiques
395, rue Wellington
Ottawa ON K1A 0N4
Canada

Your file Votre référence

Our file Notre référence

The author has granted a non-exclusive licence allowing the National Library of Canada to reproduce, loan, distribute or sell copies of this thesis in microform, paper or electronic formats.

L'auteur a accordé une licence non exclusive permettant à la Bibliothèque nationale du Canada de reproduire, prêter, distribuer ou vendre des copies de cette thèse sous la forme de microfiche/film, de reproduction sur papier ou sur format électronique.

The author retains ownership of the copyright in this thesis. Neither the thesis nor substantial extracts from it may be printed or otherwise reproduced without the author's permission.

L'auteur conserve la propriété du droit d'auteur qui protège cette thèse. Ni la thèse ni des extraits substantiels de celle-ci ne doivent être imprimés ou autrement reproduits sans son autorisation.

0-612-82270-2

Canada

University of Alberta

Library Release Form

Name of Author: *Fatih Doğan*

Title of Thesis: *Self Consistent Modification To The Electron Density Of States Due To Electron-Phonon Coupling In Metals*

Degree: *Master of Science*

Year this Degree Granted: 2003

Permission is hereby granted to the University of Alberta Library to reproduce single copies of this thesis and to lend or sell such copies for private, scholarly or scientific research purposes only.

The author reserves all other publication and other rights in association with the copyright in the thesis, and except as herein before provided, neither the thesis nor any substantial portion thereof may be printed or otherwise reproduced in any material form whatever without the author's prior written permission.

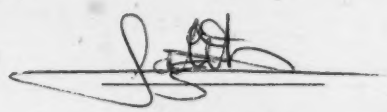

#2 *10726 84th Ave*
Edmonton, AB Canada T6E2H9

Nov 25, 2002

University of Alberta

Faculty of Graduate Studies and Research

The undersigned certify that they have read, and recommend to the Faculty of Graduate Studies and Research for acceptance, a thesis entitled **Self Consistent Modification To The Electron Density Of States Due To Electron-Phonon Coupling In Metals** submitted by **Fatih Doğan** in partial fulfillment of the requirements for the degree of Master of Science.

Frank Marsiglio (Supervisor)

Bruce Sutherland (External)

Mark Freeman

Jack Tuszynski

DATE: Oct 28, 2002

ABSTRACT

In this thesis, several assumptions made in the standard theory of electron-phonon interaction in metals, Migdal theory, are questioned. The assumption of constant density of states(DOS) with infinite bandwidth is replaced by a frequency dependant function with finite bandwidth. Due to this change, DOS is modified self-consistently with the non-zero self energy of the electron. Collapse of the band is inevitable around the phonon frequency. The collapse depends on the parameters in the problem. Details like the particular functional form of the non-interacting DOS, the characteristic width of the band compared to the characteristic phonon frequency, and the presence of other bands crossing the Fermi level quantitatively affect the outcome. However, the range over which the band spreads increases considerably for intermediate electron-phonon interaction strength. Use of general and Einstein mode spectrum are compared, and many artifacts of Einstein mode spectrum are revealed.

Acknowledgements

I would like to thank everyone from whom i learned during last two years, especially my supervisor, Frank Marsiglio for his support, encouragement and helpful discussion. The committee members for their effort. Special thanks to Lucian Covaci for his help on numerical calculations and Esin Albay for her help with figures. This thesis is to my parents. I could not have finished it without their support.

To

My Parents

Table of Contents

List of Figures

List of Tables

Chapter 1. Introduction 1

Chapter 2. Theory 11

Chapter 3. Results 19

3.1. Reproduction and Correction of Alexandrov et al. results 20

3.2. Introduction of Constant Bare Density of States 25

3.3. Effect of The Background Band For An Einstein Mode 29

3.4. Effect of the Value of Bare Bandwidth for an Einstein Mode 32

3.5. Transition from an Einstein mode to a broad spectrum 35

3.6. The center of the phonon spectrum 40

3.7. Effect of Background Band for Broad Phonon Spectrum 40

3.8. Effect of the Bare Bandwidth Value for Broad Phonon Spectrum 48

Chapter 4. Conclusions 53

Bibliography 56

Appendix A. Derivation of Density of States Equation for Specific Distributions 58

A.1. Lorentzian Bare Density of States 58

A.2. Constant Bare Density of States 60

Appendix B. Derivation of Electron Self-Energy for Specific Phonon Spectrum 61

B.1. Einstein Mode 62

B.2. Lorentzian Spectrum 63

Appendix C. An Alternative Derivation for The Electron Self-Energy 65

Appendix D. The Required Matsubara Summation 70

Appendix E. An Introduction to Green Functions 72

E.1. Dyson Equation 75

Appendix F. The Electron Self-Energy With Angular Dependence 77

List of Tables

1 Experimental mass m_{th}, band mass m_b from pseudopotential calculations, and electron-phonon mass enhancement factor $1 + \lambda$ from pseudopotential calculations[3]. 2

List of Figures

1.1 Correction to electronic dispersion curve due to screening by the ions. Source: Solid State physics, Ashcroft, N.W. and N.D. Mermin[**2**] 2

1.2 The constant bare density of states as a function of frequency normalized to characteristic phonon frequency. Arrow shows the bandwidth location used in this thesis(FWHM). 8

1.3 The Lorentzian bare density of states as a function of frequency normalized to characteristic phonon frequency. Arrow shows the bandwidth location used in this thesis(FWHM). 9

1.4 The electron-phonon coupling function for broad spectrum. 10

2.1 Diagrammatic representation of Migdal's approximation for electron self-energy 12

2.2 Second order corrections to electronic self-energy. 17

3.1 The results as it is shown in paper by Alexandrov et al.[**16**] 20

3.2 The modified density of states for $N_s = 1, D/2 = 5\omega_E$ for an Einstein mode. Unless otherwise noted, for this graph and for all density of states graphs, λ values are: 0.1(solid line),1(long dash),2(short dash), 3(dotted),4.5(long dash with dot). Inset shows modified bandwidth as a function of λ(see text). The

horizontal line shows location of bandwidth level, and vertical line shows bare bandwidth. 22

3.3 Imaginary part of self-energy for $N_s = 1, D/2 = 5\omega_E$ for an Einstein mode with Lorentzian bare density of states. 23

3.4 Real part of self-energy for $N_s = 1, D/2 = 5\omega_E$ for an Einstein mode with Lorentzian bare density of states. 24

3.5 Real part of self-energy for $N_s = 1, D/2 = 5\omega_E$ for an Einstein mode with constant bare density of states. 26

3.6 Imaginary part of self-energy for $N_s = 1, D/2 = 5\omega_E$ for an Einstein mode with constant bare density of states. 27

3.7 Real part of self-energy for $N_s = 1, D/2 = 5\omega_E$ for an Einstein mode with constant bare density of states focused on Einstein frequency. Line is $\epsilon - \omega_c$. 28

3.8 Modified density of states for $N_s = 1, D/2 = 5\omega_E$ for an Einstein mode with constant bare density of states. 29

3.9 Modified density of states for $N_s = 0.5, D/2 = 5\omega_E$ for an Einstein mode with constant bare density of states. 30

3.10 Modified density of states for $N_s = 0, D/2 = 5\omega_E$ for an Einstein mode with constant bare density of states. 31

3.11 Modified density of states for $N_s = 0.5, D/2 = 5\omega_E$ for an Einstein mode with Lorentzian bare density of states. 32

3.12 Modified density of states for $N_s = 0, D/2 = 5\omega_E$ for an Einstein mode with Lorentzian bare density of states. 33

3.13 Modified density of states for $N_s = 1, D/2 = 10\omega_E$ for an Einstein mode with constant bare density of states. 33

3.14 Modified density of states for $N_s = 0.5, D/2 = 10\omega_E$ for an Einstein mode with constant bare density of states. 34

3.15 Modified density of states for $N_s = 0, D/2 = 10\omega_E$ for an Einstein mode with constant bare density of states. 35

3.16 Modified density of states for $N_s = 1, D/2 = 10\omega_E$ for an Einstein mode with Lorentzian bare density of states. 36

3.17 Modified density of states for $N_s = 0.5, D/2 = 10\omega_E$ for an Einstein mode with Lorentzian bare density of states. 36

3.18 Modified density of states for $N_s = 0, D/2 = 10\omega_E$ for an Einstein mode with Lorentzian bare density of states. 37

3.19 Modified density of states for $N_s = 1, D/2 = 5\omega_E$ as the width of α^2F gets wider for a Lorentzian model, shown in inset. δ values are: 0.05 meV(solid line),0.1 meV(long dash),0.5 meV(short dash), 1 meV(dotted),and 0(or Einstein mode)(long dash with dot). Inset shows α^2F for corresponding non-zero width. 39

3.20 Modified density of states for $N_s = 1, D/2 = 5\omega_E$ for a Lorentzian phonon distribution at 1meV with constant bare density of states. 41

3.21 Modified density of states for $N_s = 1, D/2 = 5\omega_E$ for a Lorentzian phonon distribution at 5meV with constant bare density of states. 41

3.22 Modified density of states for $N_s = 1, D/2 = 5\omega_E$ for a Lorentzian phonon distribution at 15meV with constant bare density of states. 42

3.23 Modified density of states for $N_s = 1, D/2 = 5\omega_E$ for a Lorentzian phonon distribution at 1meV with Lorentzian bare density of states. 42

3.24 Modified density of states for $N_s = 1, D/2 = 5\omega_E$ for a Lorentzian phonon distribution at 5meV with Lorentzian bare density of states. 43

3.25 Modified density of states for $N_s = 1, D/2 = 5\omega_E$ for a Lorentzian phonon distribution at 15meV with Lorentzian bare density of states. 43

3.26 Modified density of states for $N_s = 0.5, D/2 = 5\omega_E$ for a Lorentzian phonon distribution with Lorentzian bare density of states. 44

3.27 Modified density of states for $N_s = 0, D/2 = 5\omega_E$ for a Lorentzian phonon distribution with Lorentzian bare density of states. 45

3.28 Modified density of states for $N_s = 0.5, D/2 = 5\omega_E$ for a Lorentzian phonon distribution with constant bare density of states. 46

3.29 Modified density of states for $N_s = 0, D/2 = 5\omega_E$ for a Lorentzian phonon distribution with constant bare density of states. 46

3.30 Modified density of states for $N_s = 1$(solid) and $N_s = 0.5$(dashed) $D/2 = 5\omega_E$ for a Lorentzian phonon distribution with constant bare density of states. 47

3.31 Modified density of states for $N_s = 0.5$(solid) and $N_s = 0$(dashed) $D/2 = 5\omega_E$ for a Lorentzian phonon distribution with constant bare density of states. 48

3.32 Modified density of states for $N_s = 1, D/2 = 10\omega_E$ for a Lorentzian phonon distribution with Lorentzian bare density of states. 49

3.33 Modified density of states for $N_s = 0.5, D/2 = 10\omega_E$ for a Lorentzian phonon distribution with Lorentzian bare density of states. 50

3.34 Modified density of states for $N_s = 0, D/2 = 10\omega_E$ for a Lorentzian phonon distribution with Lorentzian bare density of states. 50

3.35 Modified density of states for $N_s = 1, D/2 = 10\omega_E$ for a Lorentzian phonon distribution with constant bare density of states. 51

3.36 Modified density of states for $N_s = 0.5, D/2 = 10\omega_E$ for a Lorentzian phonon distribution with constant bare density of states. 52

3.37 Modified density of states for $N_s = 0.5, D/2 = 10\omega_E$ for a Lorentzian phonon distribution with constant bare density of states. 52

E.1 Diagrammatic representation of full Green Function 75

E.2 Diagrammatic representation of electron self-energy 76

CHAPTER 1

Introduction

In metals, there are two separate systems. In the crystal part, phonons are present due to vibrations of ions from their equilibrium states. In the valance band, electrons are highly delocalized, forming a free electron gas.

The electron-phonon interaction in metals shows itself in several properties. Phonons are influenced by the electron gas; therefore understanding phonon systems requires a correct treatment of the electron-phonon interaction. In turn, electrons around the Fermi energy are affected by phonons. The electron-phonon interaction affects the electron dispersion curve around the Fermi energy as shown in Figure 1.1. This theoretical prediction has been seen in many experiments.

In heat capacity measurements, this effect shows itself in the electronic part of the heat capacity[1]. The low temperature behavior of the heat capacity of metals can be described by:

$$C = C_e + C_{ph} = \gamma T + AT^3 \tag{1.1}$$

where C is heat capacity per mole. For the free electron gas, the coefficient of the electronic part is:

$$\gamma = \frac{\pi^2 k_B^2 N_0 m}{\hbar^2 (3\pi^2 n)^{2/3}} \tag{1.2}$$

where k_B is Boltzman constant, N_0 is Avogadro's number, m is the electron mass, $\hbar = 2\pi h$ with h being Planck's constant, n is the number of electrons per unit volume.

Writing γ with respect to quantities at the Fermi level helps to understand the

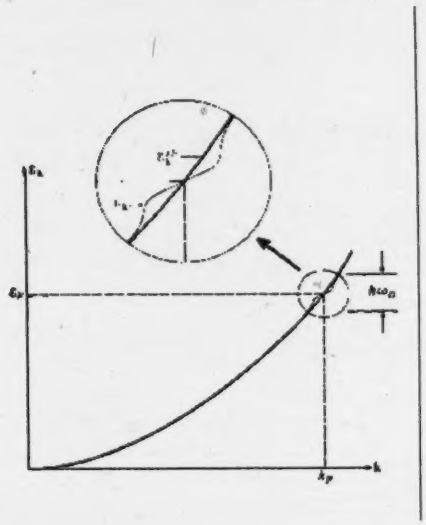

FIGURE 1.1. Correction to electronic dispersion curve due to screening by the ions. Source: Solid State physics, Ashcroft, N.W. and N.D. Mermin[**2**]

TABLE 1. Experimental mass m_{th}, band mass m_b from pseudopotential calculations, and electron-phonon mass enhancement factor $1+\lambda$ from pseudopotential calculations[**3**].

Element	m_{th}/m	m_b/m	m_{th}/m_b	$1+\lambda$
Li	2.22	1.54	1.44	1.41
Na	1.24	1.01	1.22	1.16
K	1.21	1.07	1.13	1.13
Rb	1.37	1.19	1.15	1.16
Cs	1.80	1.53	1.18	1.15
Al	1.49	1.05	1.42	1.44

effect of the electron-phonon interaction better:

$$\gamma = \gamma_b = \frac{N_b(\epsilon_F)}{N_0(\epsilon_F)}\gamma_0 = \frac{m_b}{m}\gamma_0 \tag{1.3}$$

where X_0 values are non-interacting values and X_b values are from pseudopotential calculations. From the ratio of experimental and free electron values of the electronic heat capacity coefficient, one can define the thermal effective electron mass as:

$$m_{th} = \frac{\gamma_{exp}}{\gamma_0} m \tag{1.4}$$

In Table 1, different ratios of band masses are given along with the mass enhancement coefficient, $1 + \lambda$, where λ is the electron-phonon interaction strength.

In electrical resistivity, a well known equation for the resistivity at low temperature is:

$$\rho = \frac{m}{ne^2\tau} \tag{1.5}$$

This equation can be improved by first replacing the bare mass of the electron with the band mass, then replacing the relaxation time due to impurity and phonon scattering, τ with the following approximation:

$$\rho = \frac{4\pi m_b}{ne^2}\left(\frac{1}{\tau_{imp}} + \int_0^{\omega_{max}} \frac{(\beta\omega)\alpha_{tr}^2 F(\omega)}{(e^{\beta\omega}-1)(1-e^{-\beta\omega})} d\omega\right) \tag{1.6}$$

where $\alpha_{tr}^2 F(\omega)$ is the electron-phonon coupling function relevant for transport properties. The difference from the ordinary coupling function is that this function includes angular change due to phonons because in transport properties momentum of the final state is important.

At high temperatures ($\beta\omega_{max} < 1$):

$$\rho = \frac{4\pi m_b}{ne^2\hbar\beta}\lambda_{tr} \tag{1.7}$$

where $\beta = \frac{1}{k_B T}$.

Recently, an ARPES (Angle Resolved Photo Emission Spectroscopy) experiment revealed the existence of a kink in the dispersion relation of several high temperature superconductors in the normal state[4]. This kink appears to be at the

characteristic phonon frequency of the materials. Therefore, it is thought that the reason behind the kink is the electron-phonon interaction[4][5].

BCS theory[6] and Eliashberg theory[7], which explain superconductivity in several superconductors, are applications of the electron-phonon interaction. Since this topic is a subject which is too broad to focus on here, detailed explanations are not given. The reader may refer to several references for detailed analysis of these theories[8][9].

There have been two different approaches to explain this coupling theoretically in metals. One of these approaches assumes single electron interacting with phonons. This approach is used for high electron-phonon coupling strength. The physics is based on polaron structure.

Polarons were first introduced by Landau in 1933[10]. A polaron is an electron in a conduction band of a solid where the particle density is low. The Coulomb force that one electron exerts on another electron at a distance r is $e^2/\epsilon_0 r^2$. However, if there is no movement of ions the same force would be $e^2/\epsilon r^2$, where, ϵ_0 and ϵ are static and high-frequency dielectric constants[11]. Therefore, in case of ion movement, the electron feels a potential energy of:

$$-\frac{e^2(\epsilon^{-1}-\epsilon_0^{-1})}{r}. \tag{1.8}$$

Since the potential is attractive, localized states may readily occur. The electron is 'trapped by digging its own hole'. This localized state is due to phonons affecting electrons. The localization occur in the meaning of electron getting slower, not localization in space. Because in crystals, due to Bloch's theorem, electrons are highly delocalized in space. Effective mass of the electron gets large due to the phonon cloud around the electron. The effect of phonons on a single electron and on two electrons was investigated by Marsiglio[12] and references therein.

The second approach was introduced by Migdal in 1958[13]. This approach is

used to explain the weak coupling limit. The main aspect of this approach is that an electron around the Fermi level has a self energy due to its interaction with phonons.

The self-energy concept appears in many contexts. If one takes the system with no phonons as the unperturbed state, the energy change due to the existence of phonons can be considered as a perturbation to the electronic structure[**14**]. Up to second order in electron-phonon processes, one electron, from within the Fermi surface, emits one phonon, then by absorbing the same phonon goes back to its original state. If there is one extra electron outside the Fermi surface, this extra electron affects this process in the following way. Like the electron within the Fermi surface, this electron can absorb (or emit) one phonon and then emit (or absorb) that phonon and get back to its original state. In addition to that process, the electron inside Fermi surface feels additional restrictions due to the existence of another electron through the Pauli exclusion principle. Hence, the energy of the electron is changed. The sum of these two effects gives the self-energy of the electron.

In this thesis, focus is given to second approach (often called Migdal's approximation). In the superconducting state, Migdal's approximation is generalized to Eliashberg theory which explains many superconducting materials.

Many researchers have used the Migdal approximation to explain various known properties or to predict features to be found in experiments. The theory works pretty accurately for most of the metals. However, since the theory is not exact, people have questioned the validity of the results in certain parameter regimes obtained by using Migdal theory. As one looks carefully at the derivation of the theory, many assumptions made in the derivation can be considered oversimplifications.

A major question is: for what range of the electron-phonon interaction strength,

do the assumptions made in Migdal theory hold? The theory assumes that the electron-phonon coupling is weak. This constraint is defined according to other assumptions while building the approximation through a perturbation. In this thesis, a specific assumption is questioned and the validity of the theory without that approximation is investigated. The assumption that is questioned here is the **constant density of states around the Fermi energy with infinite bandwidth.** How the existence of the electron-phonon interaction modifies the bare density of states which has finite bandwidth and is frequency dependent is the main question.

This assumption was first relaxed in the context of the Migdal approximation by Engelsberg and Schrieffer[**15**]. In that work the results were inconclusive, as the following quote reveals: "...although by taking a finite cutoff, the effects of multiple-phonon processes may be seen, their effect is too small to be considered reliable in our approximation." The results were too small because although they assumed a finite cutoff for the lower end, the cutoff was -μ, the Fermi energy, which was very large compared to characteristic phonon frequency. Here, a much narrower case will be considered (10 to 20 times the order of phonon frequency rather than 1000). In addition, in Engelsberg et al.'s work, self-consistent modification to the density of states and frequency dependence of the density of states was not included. Even with those conditions, they found changes to the Green function (and so to the self-energy), and they showed analytically that multi-phonon processes affect the self-energy. For an introduction to the Green function method, refer to appendix E.

If the bare density of states is assumed to be frequency dependant, then it is modified by the electron-phonon interaction self-consistently.

A standard approach would be to see how the removal of this approximation affects the self-energy. However, the structure of the self-energy is relatively complicated

and there are two different parts to keep track of (real and imaginary parts). Therefore, in this analysis, how the frequency dependant density of states is modified by the existence of a non-zero self-energy (self-consistently) will be discussed directly by analyzing the changes in the density of states.

This approach was first used by Alexandrov et al.[**16**] The aim was to see if the electron-phonon relation causes polaron collapse.

In the case of large electron-phonon interaction strength, existence of many phonons is expected to cause the polaronic physics to be important. As pointed out earlier, the main question is "for what value of electron-phonon coupling strength does this occur?" or "when does this effect become dominant?"

Alexandrov et al.[**16**] investigated this question and found that "...at some value of λ,$\lambda^* \geq \lambda > 1$, the bandwidth decreases sharply to $\tilde{D} < \omega$. The kinetic energy of electron decreases below characteristic phonon frequencies..." For some value of λ, of the order of 1, they found that Migdal's approximation is no longer valid. However, there are several materials with λ larger than 1, which explained by Migdal's approximation, for example Pb. Therefore, either the explanation of Pb by Migdal's approximation is not valid or results presented in their work is not.

In their paper, the effect described above is investigated for an Einstein mode (Holstein model)[**17**] which assumes that the phonon contribution can be summarized by an effective spectrum with a delta function at a particular frequency. However, due to the nature of their approach, and inaccuracies in their calculations, in that investigation, they did not see all the effects due to finite bandwidth and frequency dependant density of states.

In this thesis, their approach is revisited and has been extended for a broadened phonon spectrum. The calculations for the Einstein model are repeated with a better analytical formalism for the parameters of the problem. Then, the same analysis is carried out for a broad phonon spectrum. Qualitative and quantitative

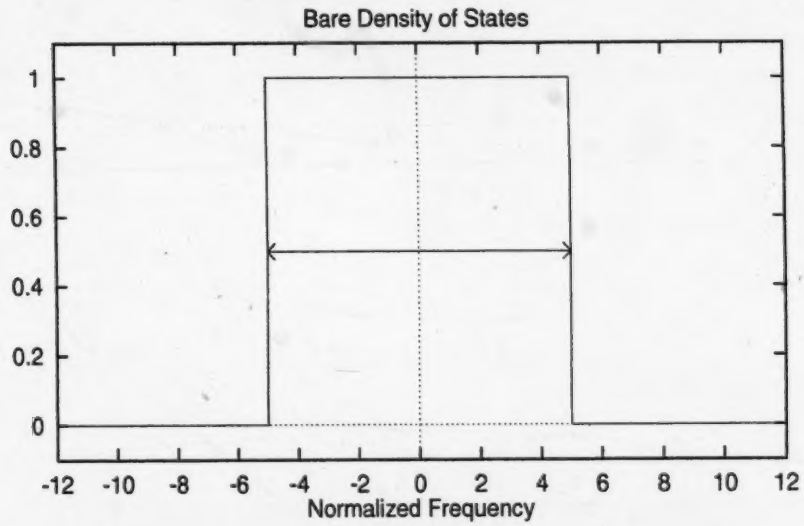

FIGURE 1.2. The constant bare density of states as a function of frequency normalized to characteristic phonon frequency. Arrow shows the bandwidth location used in this thesis(FWHM).

differences between the two phonon spectrums are described.

In the next chapter, a theoretical derivation of the Migdal's approximation with and without the "standard" approximations are given. The formalism used in the current work as a continuation from the approximation is derived in Appendix A. In chapter III, numerical calculations are described, results obtained are presented and comparisons are made. In the first section, more accurate results using the original parameters of to Alexandrov et al.[**16**] are shown and contrasted with their original results. Then, the same calculation is done for a constant bare density of states (Fig.1.2) with otherwise similar parameters. A comparison to the Lorentzian case (Fig.1.3), which is the bare density of states used previously, is given. For a complete analysis of the problem, parameters of the system are varied. The varied parameters are; the background band which is assumed to be the band with infinite bandwidth without frequency dependence, which is the band used in the

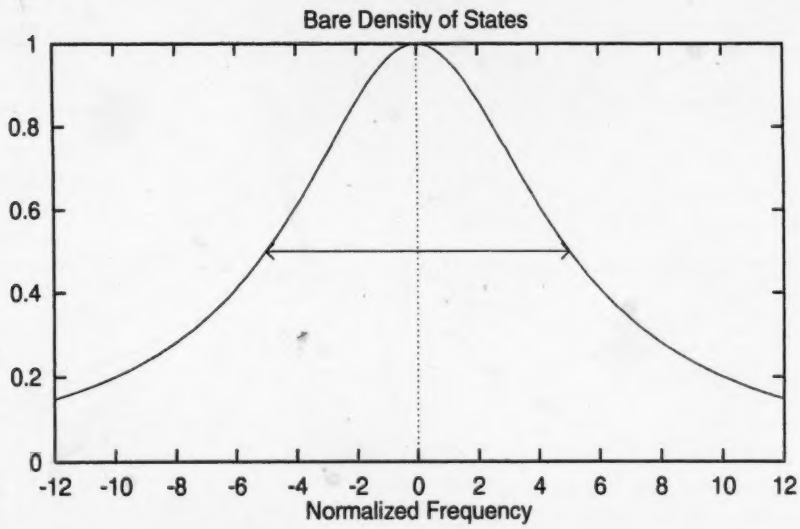

FIGURE 1.3. The Lorentzian bare density of states as a function of frequency normalized to characteristic phonon frequency. Arrow shows the bandwidth location used in this thesis(FWHM).

case of the "standard" approximation, the value of the bare bandwidth compared to a characteristic frequency of the phonon spectrum. Each case is studied for its contribution to the features in the modified density of states for both Lorentzian and constant bare densities of states. With this analysis, all features of the Einstein mode are explored for a finite bandwidth electron density of states. Next, based on the analysis of the Einstein mode, the framework is extended to a broad phonon spectrum, which is assumed to have a Lorentzian distribution (Fig 1.4). Features present with this spectrum are repeated, new features are described and artificial features of the Einstein mode are revealed.

In chapter IV, conclusions are presented with open points for more advanced analysis in the future.

For simplicity, throughout the analysis, the half filling condition will be assumed,

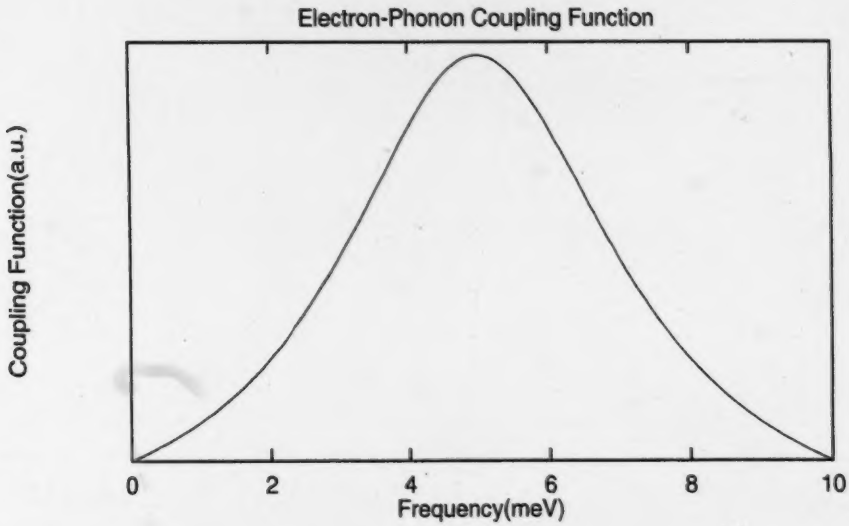

FIGURE 1.4. The electron-phonon coupling function for broad spectrum.

for which case due to particle hole symmetry, the existence of the electron-phonon interaction does not affect the Fermi energy.

CHAPTER 2

Theory

As explained in the previous section, the electron-phonon interaction can be investigated using Migdal's approximation. In this section a review of the formal derivation of the results of Migdal's approximation will be given[**20**].

The solution of the electron-phonon interaction is not trivial. Two different systems which are complicated within themselves affect each other simultaneously. Here, the electron self-energy will be calculated assuming that phonon properties are known. The structure of the electron self-energy is modified due to the electron-phonon interaction. Calculation of self-energy is relatively straightforward.

As shown in Appendix E, the full electron self-energy is described by Figure E.2b. The formula for that diagram is:

$$\Sigma(\mathbf{k}, i\omega_m) = \frac{-1}{N\beta}\sum_{q,n} g_{\mathbf{k},\mathbf{k+q}} D(\mathbf{q}, i\nu_n) G(\mathbf{k+q}, i\omega_m - i\nu_n) \Gamma(\mathbf{k+q}, \mathbf{k}, \mathbf{q}, i\omega_m, i\nu_n) \tag{2.1}$$

where $\beta = \frac{1}{k_B T}$, $i\omega_m (i\nu_n)$ is fermion (boson) Matsubara frequency, Γ is the shaded area in Figure E.2b which represents higher order corrections to the lowest order electron self-energy other than one phonon with the bare electron. However, in Migdal's approximation, it can be shown that these corrections are of the order of $(\frac{m}{M})^{1/2}$ compared to the lowest order. In other words, Γ can be written as:

$$\Gamma = g(1 + O(\frac{m}{M})^{1/2}) \tag{2.2}$$

where m(M) is electron(ion) mass. $g_{k,k+q}$ in these calculations is the matrix element defining absorption or emission of one phonon by an electron. Therefore, the

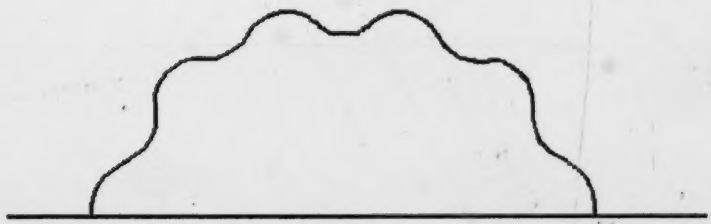

FIGURE 2.1. Diagrammatic representation of Migdal's approximation for electron self-energy

electron self-energy in the case of the electron-phonon interaction with Migdal's approximation can be described by a Feynman diagram as shown in Figure 2.1. The equation for this diagram is:

$$\Sigma(k, i\omega_m) = \frac{-1}{N\beta} \sum_{q,n} g_{k,k+q} D(q, i\nu_n) G(k+q, i\omega_m - i\nu_n) g_{k+q,k} \tag{2.3}$$

where the vertices are identified by the matrix element and higher order corrections are assumed negligible. The first step in analyzing this equation is to substitute the phonon spectrum function in place of the phonon propagator:

$$\Sigma(k, i\omega_m) = \frac{-1}{N\beta} \sum_{q,n} |g_{k,k+q}|^2 \int_0^\infty d\Omega B(\mathbf{q}, \Omega) [\frac{1}{i\nu_n - \Omega} - \frac{1}{i\nu_n + \Omega}] G(k+q, i\omega_m - i\nu_n). \tag{2.4}$$

In this equation, the phonon spectral function is multiplied by the coupling parameter. Along with the density of states at the Fermi level, this combination defines the electron-phonon spectral function:

$$\alpha^2 F(k, k', \Omega) = N(0) |g_{k,k'}|^2 B(k - k', \Omega). \tag{2.5}$$

Substituting this definition into the self-energy equation, one obtains:

$$\Sigma(k, i\omega_m) = \frac{-1}{\beta} \sum_{q,n} \int_0^\infty d\Omega \frac{\alpha^2 F(k, k+q, \Omega)}{N(0)} [\frac{1}{i\nu_n - \Omega} - \frac{1}{i\nu_n + \Omega}] G(k+q, i\omega_m - i\nu_n).$$

(2.6)

All of the analysis of this thesis assumes angular symmetry in k. Therefore only the energy contribution will be taken into account here. For the angular dependence of this function, a complete derivation is given in Appendix F. In general, the electron-phonon spectral function is averaged over the Fermi surface:

$$\alpha^2F(k,\Omega) = \langle \alpha^2F(k,k+q,\Omega)\rangle_{FS} = \sum_{k'} \frac{\alpha^2F(k,k',\Omega)}{N(0)}\delta(\epsilon_{k'}) \tag{2.7}$$

resulting in:

$$\Sigma(k,i\omega_m) = \frac{-1}{\beta}\sum_{k',n}\int_0^\infty d\Omega \frac{\alpha^2F(k,\Omega)}{N(0)}[\frac{1}{i\nu_n-\Omega}-\frac{1}{i\nu_n+\Omega}]G(\epsilon_{k'},i\omega_m-i\nu_n). \tag{2.8}$$

Using the prescription:

$$\sum_{k'} \rightarrow \int_{-\infty}^{\infty} d\epsilon N(\epsilon) \tag{2.9}$$

one can write the equation for the self-energy as:

$$\Sigma(k,i\omega_m) = \frac{-1}{\beta}\sum_{n}\int_{-\infty}^{\infty} d\epsilon \frac{N(\epsilon)}{N(0)}\int_0^\infty d\Omega\alpha^2F(k,\Omega)\frac{2\Omega}{\nu_n^2+\Omega^2}G(\epsilon,i\omega_m-i\nu_n). \tag{2.10}$$

Up to this point, no approximations are made beyond the choice of the specific Feynman diagram. Here the derivation will follow the standard treatment with approximations except for constant density of states. The first approximation is to assume that the electron-phonon spectral function is a smooth function of k. Therefore the momentum dependence of the electron-phonon function can be

dropped with the Fermi surface averaging, resulting in:

$$\Sigma(i\omega_m) = \frac{-1}{\beta}\sum_n \int_{-\infty}^{\infty} d\epsilon \frac{N(\epsilon)}{N(0)} \int_0^{\infty} d\Omega \alpha^2 F(\Omega) \frac{2\Omega}{\nu_n^2 + \Omega^2} G(\epsilon, i\omega_m - i\nu_n). \tag{2.11}$$

At this point, there is no k dependence on left hand side, therefore, k dependence on right hand side is removed as well.

This equation can be used to calculate all thermodynamical properties of electrons. However, for complete dynamical properties, analytical continuation of the self-energy to the complex plane is required. The continuation is not unique. Before changing the arguments, all Matsubara sums on the right hand side should be calculated. If one does not first do the sum and then analytically continue, the answer changes. To demonstrate this, first the Matsubara sum will be performed. To achieve this, the spectral representation of the electron Green function will be used:

$$G(\epsilon, i\omega) = \int_{-\infty}^{\infty} d\omega' \frac{A(\epsilon, \omega')}{i\omega - \omega'}. \tag{2.12}$$

Then:

$$\Sigma(i\omega_m) = \frac{1}{\beta}\sum_n \int_{-\infty}^{\infty} d\epsilon \frac{N(\epsilon)}{N(0)} \int_0^{\infty} d\Omega \alpha^2 F(\Omega) \frac{2\Omega}{\nu_n^2 + \Omega^2} \int_{-\infty}^{\infty} d\omega' \frac{A(\epsilon, \omega')}{i\omega_m - i\nu_n - \omega'}. \tag{2.13}$$

The Matsubara sum is separated as:

$$I(i\omega_m, \Omega, \omega') = \frac{1}{\beta}\sum_n \frac{2\Omega}{\nu_n^2 + \Omega^2} \frac{1}{i\omega_m - i\nu_n - \omega'}. \tag{2.14}$$

As shown in Appendix D, if the sum is carried out before continuation, this sum is equal to:

$$I(i\omega_m, \Omega, \omega') = \frac{n(\Omega) + f(-\omega')}{i\omega - \Omega - \omega'} + \frac{n(\Omega) + f(\omega')}{i\omega + \Omega - \omega'}, \tag{2.15}$$

where $n(\Omega)$ and $f(\omega)$ are the Bose and Fermi functions respectively. If the summation is carried out after continuation, one obtains:

$$I(z,\Omega,\omega') = \frac{n(\Omega) - n(z-\omega')}{z-\Omega-\omega'} + \frac{n(\Omega) + n(z-\omega') + 1}{z+\Omega-\omega'} \tag{2.16}$$

which in not bounded for large z. Baym and Mermin showed that there is a unique continuation of the self-energy for all Im$z > 0$ which is bounded[**21**]. Therefore the second result is not the correct continuation. Substituting the first result into self-energy yields, with analytic continuation:

$$\Sigma(z) = \int_{-\infty}^{\infty} d\epsilon \frac{N(\epsilon)}{N(0)} \int_0^{\infty} d\Omega \alpha^2 F(\Omega) \int_{-\infty}^{\infty} d\omega' A(\epsilon,\omega')[\frac{n(\Omega) + f(-\omega')}{z-\Omega-\omega'} + \frac{n(\Omega) + f(\omega')}{z+\Omega-\omega'}]. \tag{2.17}$$

Rearranging the equation:

$$\Sigma(z) = \int_0^{\infty} d\Omega \alpha^2 F(\Omega) \int_{-\infty}^{\infty} d\omega' \frac{N'(\omega')}{N(0)} [\frac{n(\Omega) + f(-\omega')}{z-\Omega-\omega'} + \frac{n(\Omega) + f(\omega')}{z+\Omega-\omega'}] \tag{2.18}$$

where

$$N'(\omega') = \int_{-\infty}^{\infty} d\epsilon N(\epsilon) A(\epsilon,\omega'). \tag{2.19}$$

Since the density of states always appears as normalized to its value at the Fermi level, from this point forward, the normalized density of states will be denoted by $N_0(\epsilon)$, and the modified density of states with normalization as $N(\epsilon)$. In the standard approximation, there are two different approximations which yield same result. The first one is when the density of states is assumed to be constant with the Fermi level value, and therefore $N(\epsilon)$ is always 1. With this approximation, the spectral function integral gives unity even for the fully interacting spectral function from equation 2.19, and the standard result is reached. The second approximation is to set the electron spectral function equal to the non-interacting one, thereby

replacing it by a delta function. In this case, the modification to the density of states, and hence to the self-energy, due to the frequency dependence of the density of states cannot be observed completely, because the interaction is no longer self-consistent. In general, the spectral function is kept as the full one but the density of states is approximated. Then it is shown that having full or non-interacting spectral function does not change the result. Therefore non-interacting spectral function is used.

To complete the theoretical derivation, results for the standard approximations will be given.

When a constant density of states and/or the non-interacting spectral functions are substituted into the self-energy equation, the result is:

$$\Sigma(z) = \int_0^\infty d\Omega\alpha^2F(\Omega)\int_{-\infty}^\infty d\omega'[\frac{n(\Omega)+f(-\omega')}{z-\Omega-\omega'}+\frac{n(\Omega)+f(\omega')}{z+\Omega-\omega'}]. \quad (2.20)$$

In the complex plane, the regime of interest is the real axis. However, the self-energy is not continuous if one crosses the real axis. The self-energy just above the real axis, with small positive imaginary part, is called the retarded self-energy, and below the real axis it is called the advanced self-energy. Here, and in general, the focus is given to the retarded self-energy. At zero temperature, the Bose function is zero and the Fermi function is a step function. Therefore the retarded self-energy becomes:

$$\Sigma(\omega+i\delta) = \int_0^\infty d\Omega\alpha^2F(\Omega)ln|\frac{\omega+i\delta-\Omega}{\omega+i\delta+\Omega}|, \quad (2.21)$$

and for an Einstein mode at frequency ω_E with weight $\frac{\lambda\omega_E}{2}$:

$$\Sigma(\omega+i\delta) = \frac{\lambda\omega_E}{2}ln|\frac{\omega+i\delta-\omega_E}{\omega+i\delta+\omega_E}|. \quad (2.22)$$

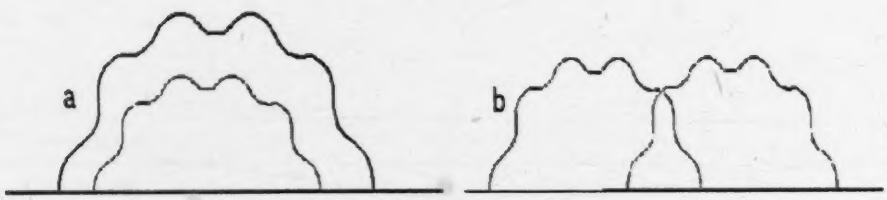

FIGURE 2.2. Second order corrections to electronic self-energy.

With the Einstein mode, the logarithm result is singular for the real part and discontinuous for the imaginary part:

$$Re\Sigma(\omega + i\delta) = \frac{\lambda\omega_E}{2} ln|\frac{\omega - \omega_E}{\omega + \omega_E}|, \tag{2.23}$$

$$Im\Sigma(\omega + i\delta) = -\frac{\pi\lambda\omega_E}{2}(\theta(\omega - \omega_E) + 1 - \theta(\omega + \omega_E)). \tag{2.24}$$

In addition to these approximations, the starting point shows why this approximation is a weak coupling approximation. The formation of the solution is based on only one Feynman diagram which assumes one phonon with dressed electron with fully interacting Green function. However, in the full analysis, all levels of interaction should be included. In Figure 2.2, second order corrections are shown. Figure 2.2a is included in this analysis since the Green function used here is the fully interacting Green function. In the fully interacting Green function, both the bare electron and the bare electron with a phonon are included. The correction in Figure 2.2a is another phonon on a dressed electron, therefore it is included. However, Figure-2.2b is not involved in this analysis. Figure-2.2a is involved in this analysis through self-consistency (not in general). For the full result, all interactions which form an infinite sum of diagrams, should be analyzed. In his paper, Migdal showed that the contribution from Figure-2.2b is smaller than the contribution from Figure-2.2a by a factor of $(\frac{m}{M})^{1/2}$ where m(M) is electron (ion)

mass. Therefore, it can be neglected for the analysis of the electron-phonon interaction. This is the basic assumption of Migdal's "theorem" which makes this approximation relatively simple to handle.

CHAPTER 3

Results

It would be appropriate to start with what variables are used in this analysis. Variables are chosen in a way that shows how certain changes from constant infinite bandwidth to a possibly frequency dependant bare density of states occur with non-zero self-energy for different coupling strength of the electron-phonon interaction. The required formalism for the analysis is given in Appendix A. Specific parts of this analysis will be done to clarify the dependence on specific parameters of this particular system:

- To compare the results to those given by Alexandrov et al.[**16**] both delta function (Einstein mode) and finite width distribution of electron-phonon interaction are used.
- In order to differentiate the effect of finite bandwidth and frequency dependence, both constant and frequency dependant (with Lorentzian distribution) bare density of states are used.
- To illustrate the continuation from infinite to finite bandwidth, two different bandwidths are used. Namely, the bandwidth is either ten times the phonon frequency or twenty times the phonon frequency.
- To use a more suitable distribution of phonons and to clarify the transition and why the Einstein mode produces artifacts which should not be present for a realistic, broad, distribution of electron-phonon interaction. Different widths of Lorentzians are used for the phonon spectrum, and the best suitable one is chosen.

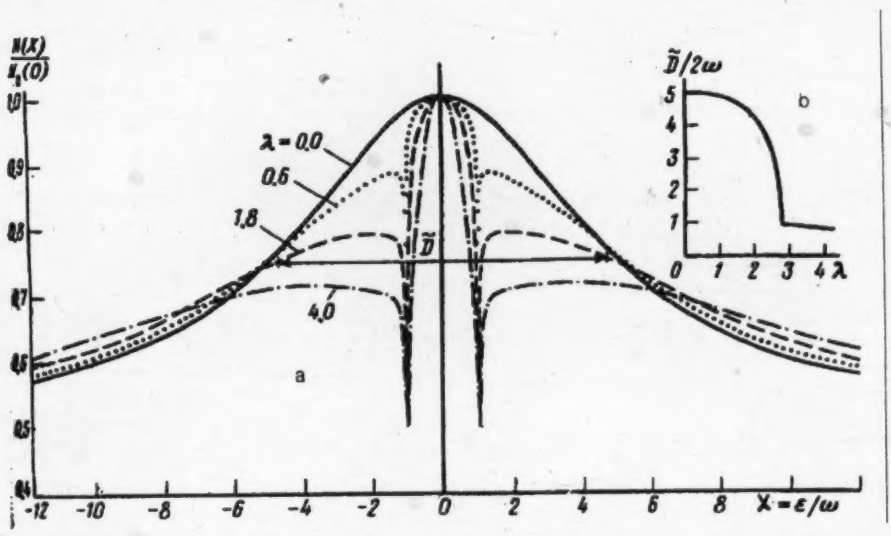

FIGURE 3.1. The results as it is shown in paper by Alexandrov et al.[16]

- To see if the absolute location of the center of the electron phonon spectral function affects the results, three different energies, 1 meV, 5 meV and 15 meV, are used as the center.
- To see how the effect of electron-phonon interaction is reflected by presence of a second band, the background band is modified to increase or decrease the overall contribution of the finite band. The background band is defined to be the effective average band including all other bands, extending from -∞ to +∞ with no frequency dependence. It is the band used in the standard approximation. Here the influence of a second band on the Migdal theory is investigated.

3.1. Reproduction and Correction of Alexandrov et al. results

In their paper, Alexandrov et al.[16] propose that the density of states with finite bandwidth causes polaron collapse for $\lambda \geq 1$. Their results are shown in Figure-3.1. However, as shown in Appendix B, the form of real part of self-energy

is:

$$Re\Sigma(\omega) = \frac{\lambda\omega_E}{2}(-2\omega\int_0^\infty d\epsilon' \frac{N(\epsilon') - N(\omega-\omega_E)}{(\epsilon'+\omega_E)^2-\omega^2} + N(\omega-\omega_E)ln|\frac{\omega-\omega_E}{\omega+\omega_E}|) \tag{3.1}$$

From this equation, it is clear that for an Einstein mode, with non-zero electron-phonon interaction strength (λ), the real part of the self-energy approaches infinity as the frequency approaches the Einstein frequency, ω_E. Since the equation for the modified density of states from Appendix A is

$$N(\epsilon) = \frac{1}{1+N_s}(\frac{D/2(D/2+|Im\Sigma(\epsilon)|)}{(Re\Sigma(\epsilon)-\epsilon)^2+(|Im\Sigma(\epsilon)|+D/2)^2} + N_s), \tag{3.2}$$

when the real part of the self-energy ($Re\Sigma(\epsilon)$) is infinite, the contribution from the band of interest to the total density of states is zero. Therefore, whatever the level of interaction is, the density of states from the band of interest is zero for the Einstein frequency provided that the electron-phonon interaction strength is not zero. As shown in Figure-3.2 (see [**22**] for a discussion of technical details), increasing the strength of the electron-phonon interaction only increases the region which the singularity affects. This means that for that point, the band ends for a short energy region. Due to the frequency dependence of the bare density of states, the total collapse occurs only at one frequency, the Einstein frequency. In the following sections more drastic examples of this collapse are given. The reader should note that the analysis given here focuses on positive energies. Particle-hole symmetry and a symmetric bare density of states guarantee that the total density of states is symmetric as well. Negative energies can be deduced by simply taking a symmetric vertical reflection on the Fermi energy, denoted by 0 energy here.

Another interesting difference compared to the results shown in Alexandrov et al's work was the restoration (or a peak) at nω_E. The reason for this is mainly the shape of the imaginary part of the self-energy. The imaginary part of the self-energy is

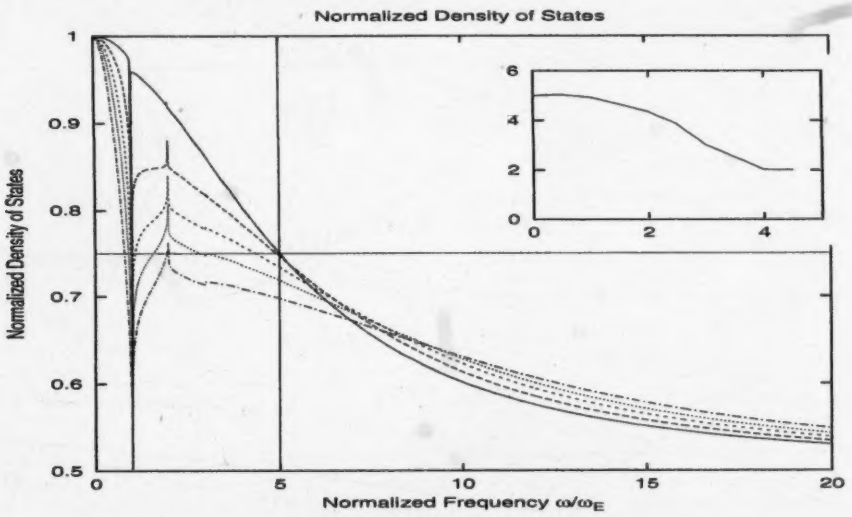

FIGURE 3.2. The modified density of states for $N_s = 1, D/2 = 5\omega_E$ for an Einstein mode. Unless otherwise noted, for this graph and for all density of states graphs, λ values are: 0.1(solid line),1(long dash),2(short dash), 3(dotted),4.5(long dash with dot). Inset shows modified bandwidth as a function of λ(see text). The horizontal line shows location of bandwidth level, and vertical line shows bare bandwidth.

related to the density of states as:

$$Im\Sigma(\epsilon) = -\frac{\pi\lambda\omega_E}{2}(N(\epsilon-\omega_E)\theta(\epsilon-\omega_E)+N(\epsilon+\omega_E)(1-\theta(\epsilon+\omega_E))), \quad (3.3)$$

where $\theta(x)$ is the Heaviside step function defined as:

$$\theta(x) = \begin{cases} 0;\ x<0 \\ 1;\ x>0 \end{cases}. \quad (3.4)$$

For positive frequencies, the second part of equation 3.3 is always zero because the step function always gives 1. The singularity of the density of states affects the imaginary part of the self-energy with a shift of ω_E. As shown in Figure 3.3, the imaginary part is similar to the density of states with slight modifications with a

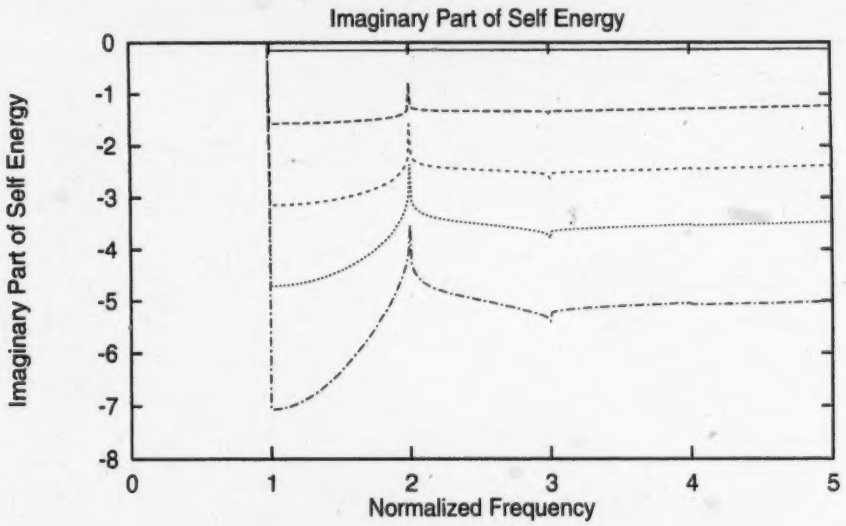

FIGURE 3.3. Imaginary part of self-energy for $N_s = 1, D/2 = 5\omega_E$ for an Einstein mode with Lorentzian bare density of states.

shift of ω_E. The behavior of the density of states at ω_E affects the imaginary part of the self-energy at $2\omega_E$. From the equation of the modified density of states, equation 3.2, it is clear that, if all variables are kept constant, the imaginary part of the self-energy modifies the width of the Lorentzian. Therefore, as the imaginary part gets larger in magnitude, keeping in mind that it is always non-positive, the modified density of states for that energy decreases. Mathematically, as the imaginary part gets larger in magnitude, the denominator of equation 3.2 grows faster than the numerator, effectively decreasing the total density of states, and when the imaginary part approaches zero, the modified density of states is restored to its original level. Another reason for this to happen can be seen through the Kramers-Kronig relations of the self-energy. "The Kramers-Kronig relation Re[Σ] and Im[Σ] guarantees that Re[Σ] has a dip when Im[Σ] has a jump" [**19**] and vice versa. Finally, the self-energy of the electron at any frequency depends on the multiples of the characteristic phonon frequency as shown in Appendix C. All these

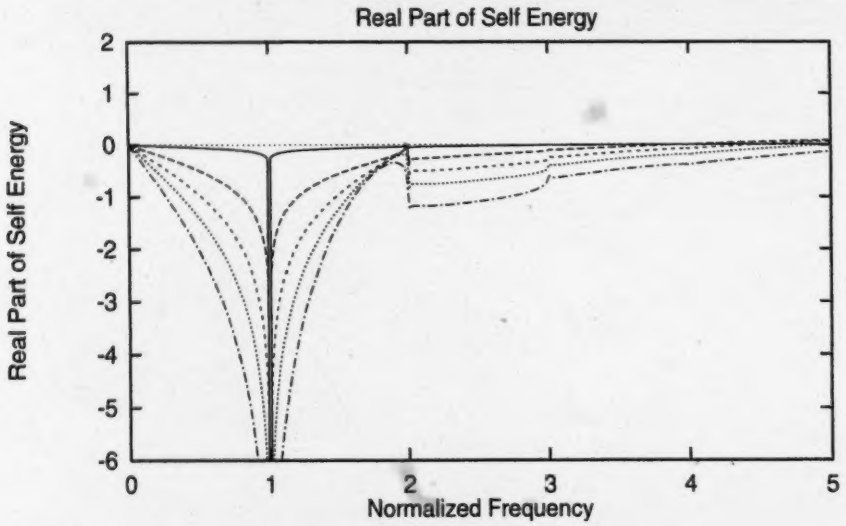

FIGURE 3.4. Real part of self-energy for $N_s = 1, D/2 = 5\omega_E$ for an Einstein mode with Lorentzian bare density of states.

effects can be seen in Figure 3.3 and Figure 3.4. Up to $2\omega_E$, the real part goes from negative infinity to zero, changing the effective center of the Lorentzian in Equation 3.2. The same argument can be made for $3\omega_E$ point for very less effective changes due to the imaginary part being affected by the density of states at $2\omega_E$ and the real part of the self-energy being almost constant. Those points will be important for future analysis of an Einstein mode.

In their paper, Alexandrov et al.[**16**] define modified bandwidth as the frequency where the band of interest drops to half its value at the Fermi energy. Due to lack of a better definition, the same definition will be used here as well. The definition of bandwidth, even for the bare density of states, does not show properly where the band ends. For example, for a Lorentzian shape, there is a considerable portion of the density of states beyond that point. In addition, as the electron-phonon interaction becomes stronger, the high energy portion of the band become enhanced, i.e. gets more important. These modifications are not taken into account in the

calculation of modified bandwidth to avoid unintentional complications. With the corrections made to Alexandrov et al.'s results, the modified bandwidth vs. λ graph shows interesting new features as shown in the inset of Figure 3.2. First of all, for small values of λ, there is an enhancement to the modified bandwidth which is not obvious because it is there only for a short range of λ. The enhancement is caused by the loss of density of states at lower energies. For a given λ, the electron-phonon interaction suppresses the density of states mainly around the phonon frequency due to single phonon processes and at higher energies due to multiple phonons. Since the density of states obeys a sum rule, the missing states must move to other energies, at higher frequencies. For a small interaction strength, suppression does not affect states as high as the bandwidth, and therefore an enhancement can be seen. However, as λ increases, the range over which suppression occurs increases. For intermediate values of λ, original bandwidth is restored due to small multi-phonon effects. As λ increases, the suppression becomes dominant and the modified bandwidth decreases. For large values of λ, results given in Alexandrov et al. show that the modified bandwidth drops to the Einstein frequency. This does not happen for the calculations described here due to the fact that the restoration (or peak) at $2\omega_E$ prevents the bandwidth from dropping below that frequency. The actual form is given as an inset in Figure 3.2. The enhancement at intermediate values of λ is barely noticeable. Such enhancement is shown for a 2D lattice structure by Marsiglio[18].

3.2. Introduction of Constant Bare Density of States

At this point it would be appropriate to do the same analysis for a constant bare density of states. For this part of the analysis, all variables are kept as before except that the bare density of states is replaced with a constant one with the same bare bandwidth. For this particular case, features are more apparent. As shown

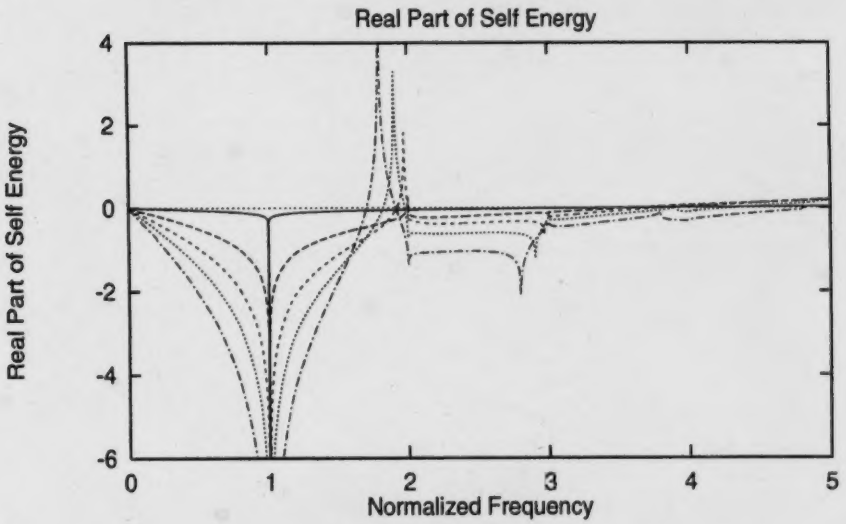

FIGURE 3.5. Real part of self-energy for $N_s = 1, D/2 = 5\omega_E$ for an Einstein mode with constant bare density of states.

in Appendix A, the complete density of states is given by the expression:

$$N(\epsilon) = \frac{1}{\pi}\frac{1}{1+N_s}(\arctan(\frac{Re\Sigma(\epsilon)+\omega_c-\epsilon}{|Im\Sigma(\epsilon)|})-\arctan(\frac{Re\Sigma(\epsilon)-\omega_E-\epsilon}{|Im\Sigma(\epsilon)|})+\pi N_s). \tag{3.5}$$

There is a point which should be cleared before further analysis. The self-energy expressions given above, equations 3.1 and 3.3, are general for any bare density of states, and therefore are valid for this part of the analysis as well. They are derived for any density of states with a specific phonon spectrum, which is an Einstein mode for this particular case. Therefore, it is clear that the logarithmic singularity in the real part of the self-energy and the discontinuity in the imaginary part which were present for the Lorentzian density of states are present in this case as well, as seen in Figures 3.5 and 3.6. However, the effect is somewhat different in this case. The argument of arctangent has zero in the denominator for energies lower than the Einstein frequency. Zero denominator prevents the real part of the

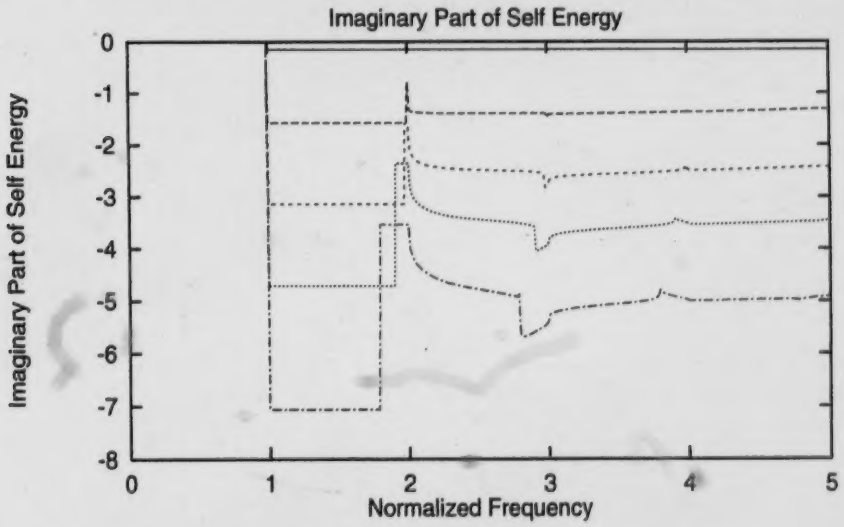

FIGURE 3.6. Imaginary part of self-energy for $N_s = 1, D/2 = 5\omega_E$ for an Einstein mode with constant bare density of states.

self-energy from modifying the density of states at low energy. At ω_E, in addition to the zero in the denominator, the numerator approaches negative infinity. This combination ensures that at the Einstein frequency, the density of states due to this band completely disappears. In addition, a new feature appears due to the fact that the imaginary part of self-energy is zero up to ω_E. Since the denominators for arctangent functions are zero, the criteria which decides whether the function gives -$\pi/2$ or +$\pi/2$ is the sign of numerator. Focusing on positive energies, for all values, the numerator of the second arctangent is negative, therefore resulting in -$\pi/2$. The first one changes sign. Depending on the sign of $Re\Sigma(\epsilon) + \omega_c - \epsilon$, the resulting density of states changes. As shown in Figure 3.7, $Re\Sigma(\epsilon)$ crosses $\epsilon - \omega_c$ line at different points depending on the strength of electron-phonon interaction. At that point the first arctangent changes sign, changing the result from +$\pi/2$ to -$\pi/2$ for that part. Both arctangents are then -$\pi/2$, and therefore the density of

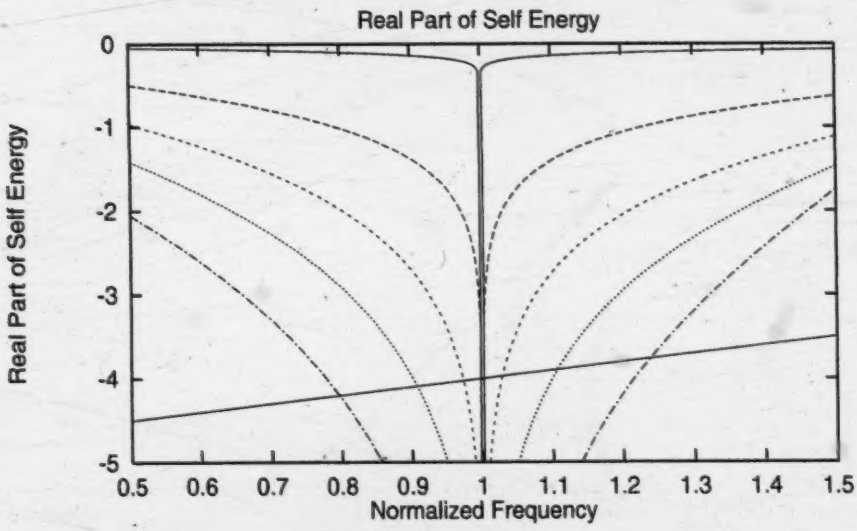

FIGURE 3.7. Real part of self-energy for $N_s = 1, D/2 = 5\omega_E$ for an Einstein mode with constant bare density of states focused on Einstein frequency. Line is $\epsilon - \omega_c$.

states due to that band collapses until ω_E, where the imaginary part of the self-energy is no longer zero and the arguments of both arctangents are finite. This feature can be considered as a real collapse of the band, since the band disappears for some range of frequencies. However, the reader should keep in mind that all these results are presented for the Einstein mode, and one of the main purposes of this thesis is to prove that usage of the Einstein mode produces artificial features which disappear for more physical phonon modes.

This crossover does not depend on the background band, but depends on the strength of the electron-phonon interaction and the bare bandwidth. Right after the Einstein frequency, the imaginary part of the self-energy is nonzero, and therefore the band is restored up to some point. At $n\omega_E$, multi-phonon effects show themselves. Since the depth at ω_E is more apparent compared to the Lorentzian case, features at $n\omega_E$ are stronger. With these features, the total density of states

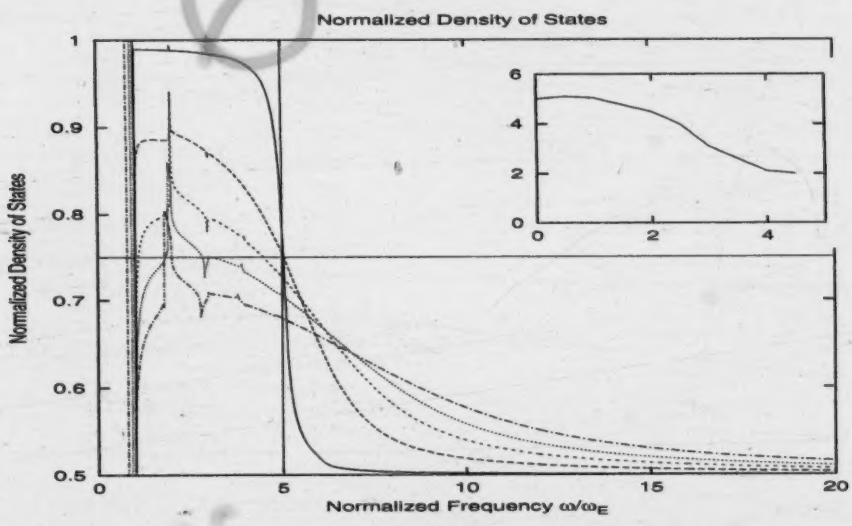

FIGURE 3.8. Modified density of states for $N_s = 1, D/2 = 5\omega_E$ for an Einstein mode with constant bare density of states.

is given in Figure 3.8. For the modified bandwidth, the enhancement is more obvious since it extends up to $\lambda = 1$. The arguments given for the Lorentzian case for the modified density of states at $\omega = 2\omega_E$ are valid for this case as well. The complete dependence is given as an inset in Figure 3.8.

3.3. Effect of The Background Band For An Einstein Mode

The complete picture is not clear for this choice of parameters, because the density of states is not completely gapped, that is, the background band is still present and prevents the density of states from disappearing. To understand this feature better, a reduction of the background band is required. In Figures 3.9 and 3.10, the background is reduced to give one third of the total states at Fermi level in the former and no contribution in the latter. For Figure 3.9, it is important to note that the peak around $2\omega_E$ actually starts at lower frequencies, which is a result of the decrease forming lower than ω_E. As described earlier, the peak is mainly due to the imaginary part of the self-energy, which depends on the density

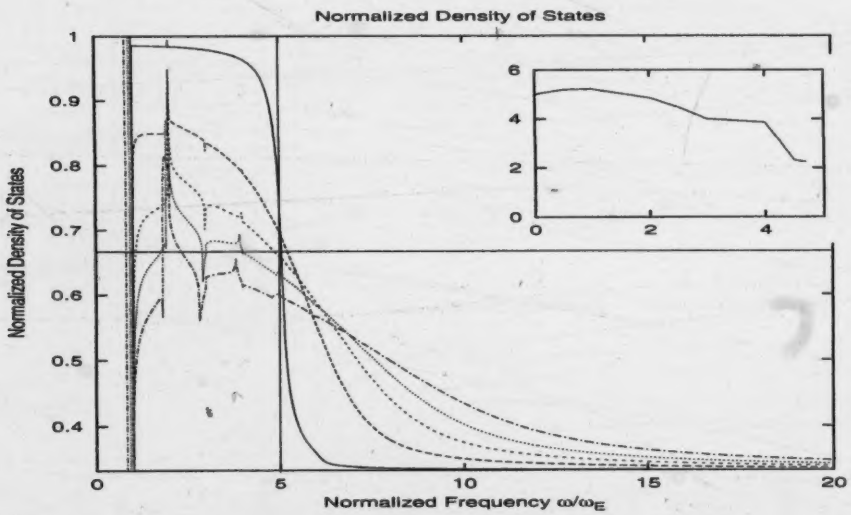

FIGURE 3.9. Modified density of states for $N_s = 0.5, D/2 = 5\omega_E$ for an Einstein mode with constant bare density of states.

of states with a shift of ω_E. Another interesting point is that, right before the peak, the value of the density of states falls. This feature is barely noticeable for $N_s = 1$. The reason for this fall at $2\omega_E$ is that for that point $Re\Sigma(\epsilon) + \omega_c - \epsilon$ has the same sign as $Re\Sigma(\epsilon) - \omega_c - \epsilon$. Since the imaginary part is not zero for that point, the effect is not as extreme. However, a reduction for that point is observable. This feature becomes apparent for $N_s = 0$ since the imaginary part goes to zero for this case, as seen in Figure 3.10. For the modified bandwidth, the decreasing background band increases the range of enhancement up to $\lambda = 4.5$ for the $N_S = 0$ case. The bandwidth does not fall below $4\omega_E$ due to a high multi-phonon enhancement at $4\omega_E$. However, the definition of bandwidth is questionable, because the band is divided into several parts. One can argue that the band ends at ω_E since the density of states is zero for a short range of energies. For large values of λ, the band around the phonon frequency collapses almost completely. However the enhancement at higher frequencies keeps the bandwidth around the

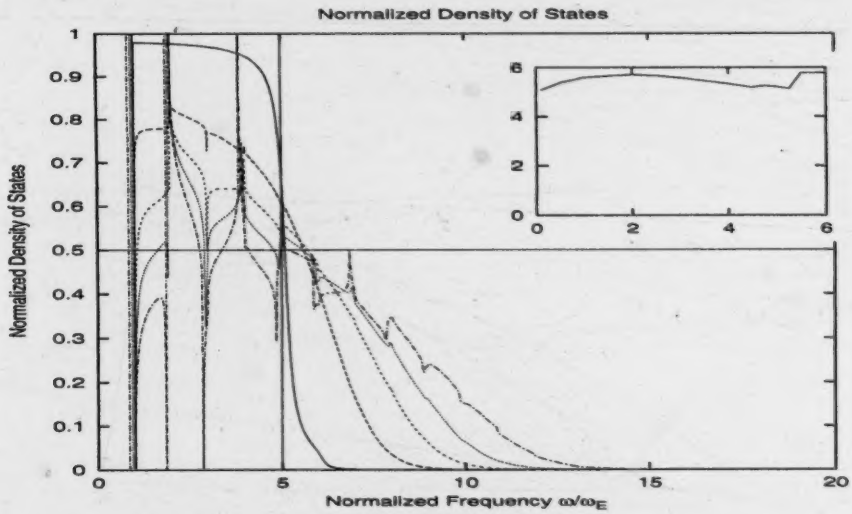

FIGURE 3.10. Modified density of states for $N_s = 0, D/2 = 5\omega_E$ for an Einstein mode with constant bare density of states.

bare bandwidth value. Because of these unphysical conditions, the modification of bandwidth due to λ shows strange features as shown in the inset of Figure 3.10. At higher frequencies, extra features are present. One of these features is the slight bump at $6\omega_E$ for $\lambda = 0.1$. The self-energy, equation 3.1, is mainly given by the average contribution from the density of states at a frequency ω_E lower than frequency of interest and integral with main contribution from energies ω_E lower than energy of interest again. For this particular frequency ($6\omega_E$), the contributing density of states is much higher than neighbor high energy scales($7\omega_E$ or $8\omega_E$ for instance), therefore enhancing the value at that range.

A similar analysis applies when the background band is varied for the frequency dependant, Lorentzian, bare density of states in Figures 3.11 and 3.12. The peak at $2\omega_E$ forms nicely as expected. It is again mainly due to shifted dependence of the imaginary part of the self-energy on the density of states. However, since the functional form is not as drastic as the constant case, no gap is observed. The

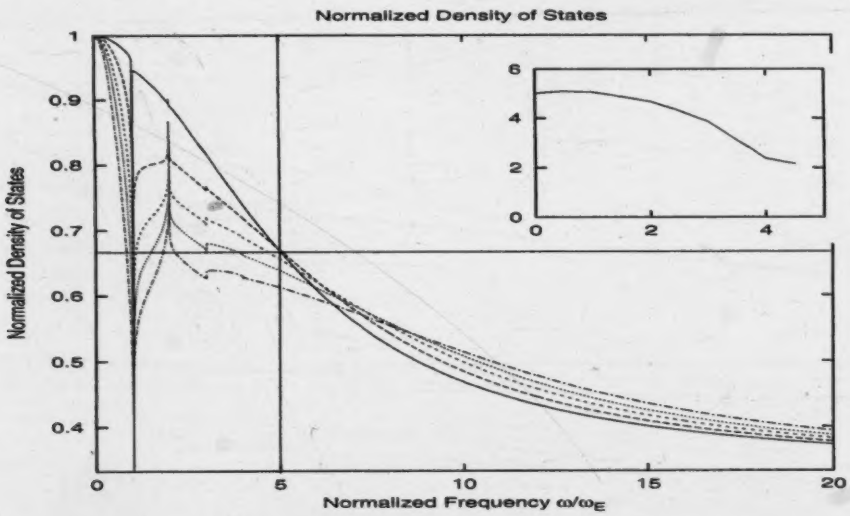

FIGURE 3.11. Modified density of states for $N_s = 0.5, D/2 = 5\omega_E$ for an Einstein mode with Lorentzian bare density of states.

enhancement of the modified bandwidth becomes more visible. Enhancement goes up to $\lambda = 3$. However, as shown in the inset of Figure 3.12, there is an obvious jump from $4\omega_E$ to $2\omega_E$. This jump is due to the enhancement at $4\omega_E$ which is not strong enough to keep itself for very high λ.

3.4. Effect of the Value of Bare Bandwidth for an Einstein Mode

To complete the analysis for the Einstein mode, we investigate how the features described above show up if the bandwidth is increased to $20\omega_E$ as in Figure 3.13. For the constant density of states, the gap is less compared to the original one. In general, the structures in the modified density of states discussed so far become weaker with increasing bandwidth. The overall effect of increasing the bare bandwidth is to decrease the effect of the electron-phonon interaction. In other words, by increasing the bare bandwidth, the effective electron-phonon interaction strength causing the modification to the density of states has been reduced. To explain this in a more conventional way, one may consider the phonon spectrum

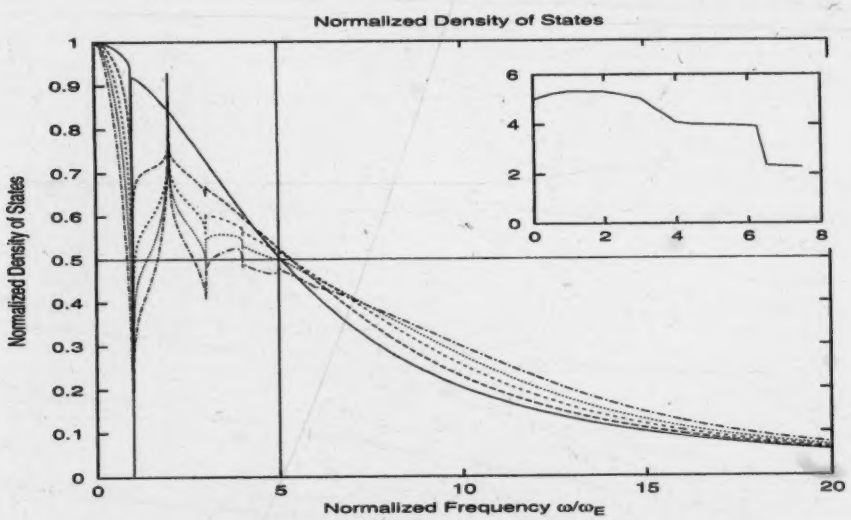

FIGURE 3.12. Modified density of states for $N_s = 0, D/2 = 5\omega_E$ for an Einstein mode with Lorentzian bare density of states.

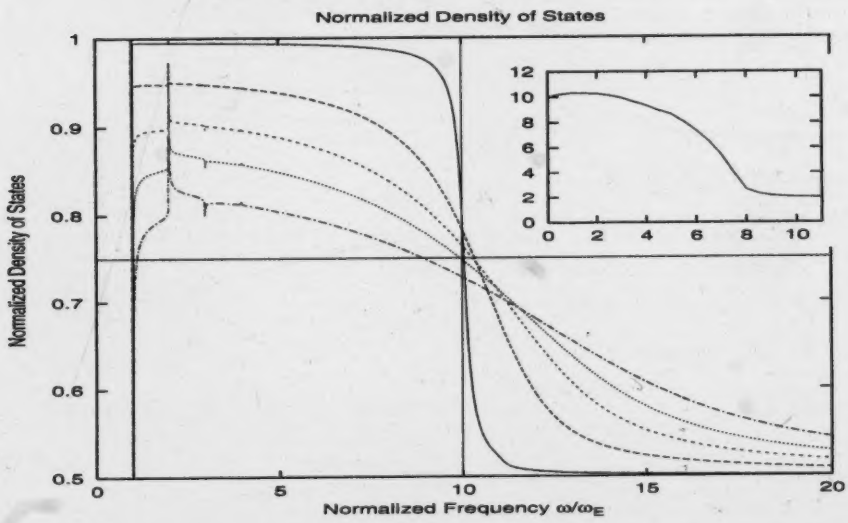

FIGURE 3.13. Modified density of states for $N_s = 1, D/2 = 10\omega_E$ for an Einstein mode with constant bare density of states.

function $\alpha^2 F$. Increasing the bare bandwidth is identical in any equation describing the density of states to decreasing the phonon frequency while keeping the bare

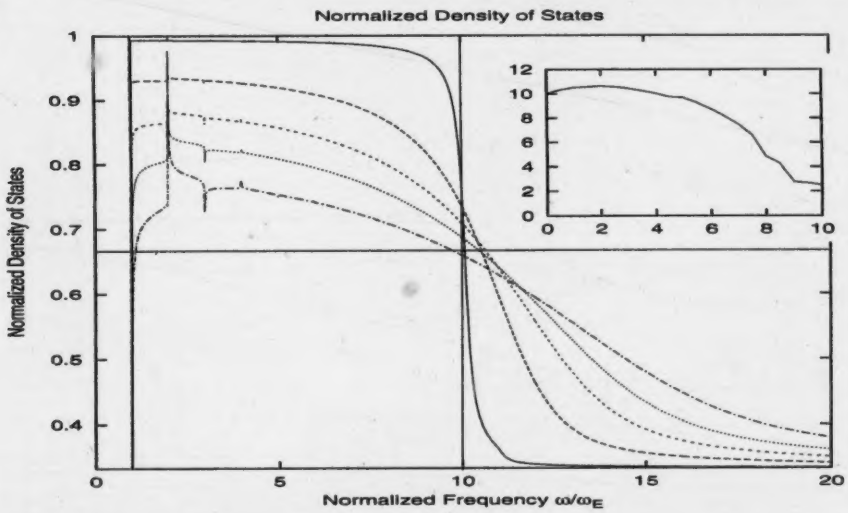

FIGURE 3.14. Modified density of states for $N_s = 0.5, D/2 = 10\omega_E$ for an Einstein mode with constant bare density of states.

bandwidth to its original value. In this case, for the same electron-phonon interaction strength, λ, the area of α^2F is reduced, effectively reducing the interacting electron-phonon strength. Since the effective interaction is less, the structures in the density of states are less pronounced. The same conclusion is true for different background bands as seen in Figures 3.14 and 3.15. This result is consistent with the observation that in the case of constant density of states with infinite bandwidth no modification is present.

This choice of bare bandwidth makes it easier to see the small λ part of the modified bandwidth. The enhancement is apparent even for $N_s = 1$. The range of enhancement is $\lambda = 2.5$ with background band, increasing up to $\lambda = 4$ with no background band. As is the case for $10\omega_E$ bare bandwidth, with no background band, the jumps get extreme at high λ values, and makes the definition of the modified bandwidth not very meaningful.

For the Lorentzian case, the same conclusions are valid about the relation between

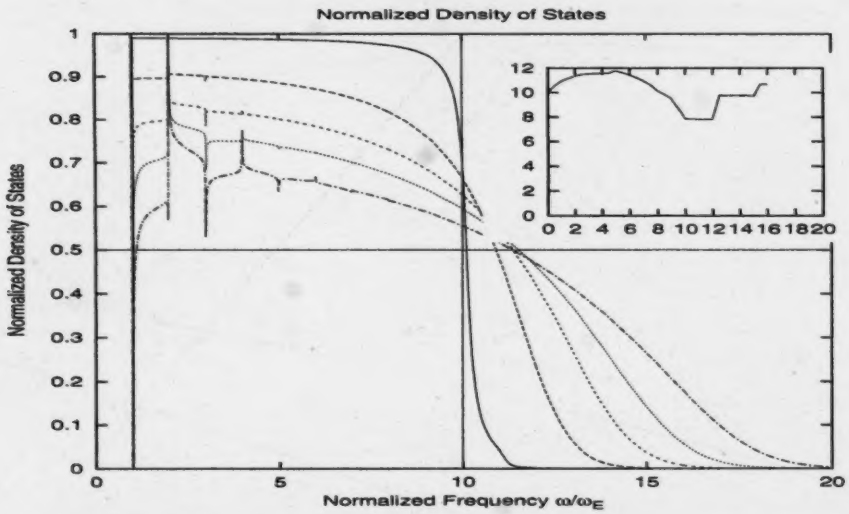

FIGURE 3.15. Modified density of states for $N_s = 0, D/2 = 10\omega_E$ for an Einstein mode with constant bare density of states.

the bare bandwidth and the electron-phonon interaction strength. The modified bandwidth enhancement range doubles with doubling of bare bandwidth, keeping the normalized range constant, as shown in Figures 3.16, 3.17 and 3.18.

3.5. Transition from an Einstein mode to a broad spectrum

It is possible that the very existence of most of the features described above is due to the fact that in the analysis an Einstein mode is used for the phonon spectrum. Features are expected to be smeared out with a broad phonon spectrum. First of all, the logarithmic singularities discussed so far are no longer present. For a general phonon spectrum, the real part of the self-energy is:

$$Re\Sigma(\epsilon) = \int_0^\infty d\omega\alpha^2F(\omega)(-2\epsilon\int_0^\infty d\epsilon'\frac{N(\epsilon') - N(\epsilon-\omega)}{(\epsilon'+\omega)^2-\epsilon^2} + N(\epsilon-\omega)ln|\frac{\epsilon-\omega}{\epsilon+\omega}|), \tag{3.6}$$

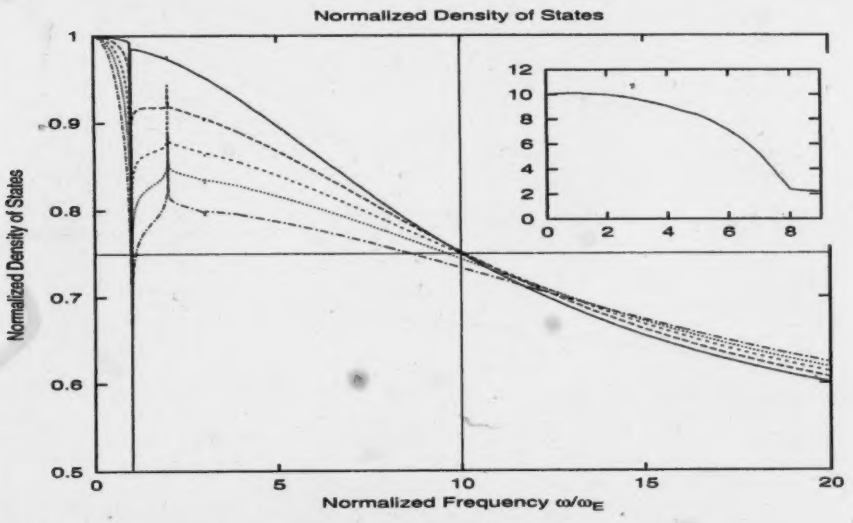

FIGURE 3.16. Modified density of states for $N_s = 1, D/2 = 10\omega_E$ for an Einstein mode with Lorentzian bare density of states.

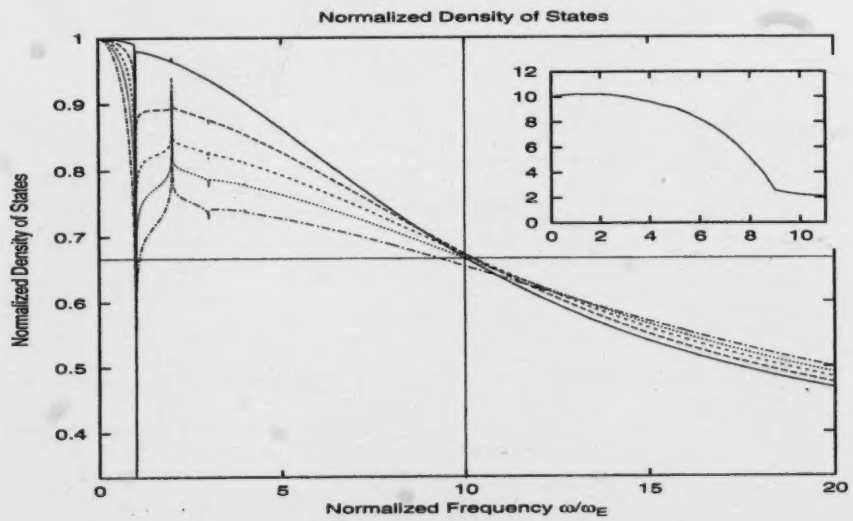

FIGURE 3.17. Modified density of states for $N_s = 0.5, D/2 = 10\omega_E$ for an Einstein mode with Lorentzian bare density of states.

and the imaginary part is:

$$Im\Sigma(\epsilon) = -\pi \int_0^\infty d\omega \alpha^2 F(\omega)(N(\epsilon-\omega)\theta(\epsilon-\omega) + N(\epsilon+\omega)(1-\theta(\epsilon+\omega))).$$

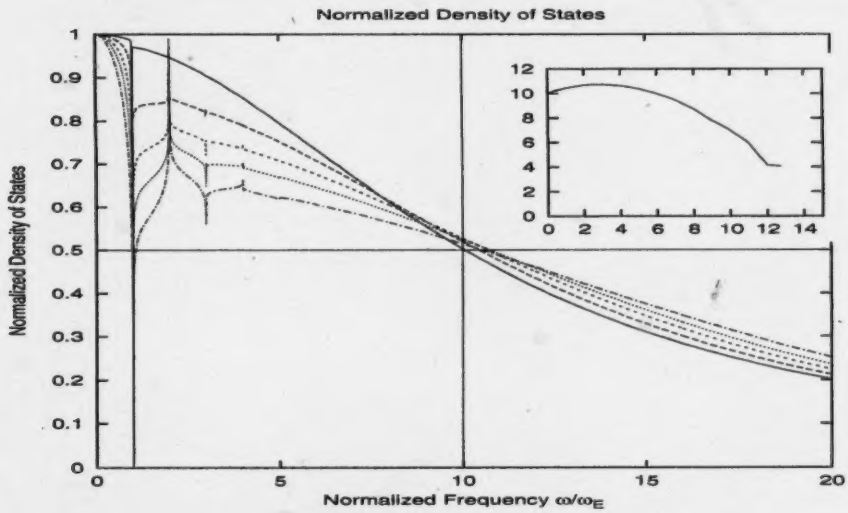

FIGURE 3.18. Modified density of states for $N_s = 0, D/2 = 10\omega_E$ for an Einstein mode with Lorentzian bare density of states.

(3.7)

Again, the second part in the integral of the imaginary part is always zero for positive frequencies, and the step function in the first part sets an upper limit for the integral, resulting in (for $\epsilon > 0$):

$$Im\Sigma(\epsilon) = -\pi \int_0^{\epsilon} d\omega \alpha^2 F(\omega) N(\epsilon - \omega) \tag{3.8}$$

which is not zero for a given frequency, provided that $\alpha^2 F(\omega)$ has nonzero values up to that frequency. One can integrate over the singularity in the real part of the self-energy, and get a finite result. Since the imaginary part is non-zero and the real part is no longer infinite, the singularity in the density of states is no longer present. To get a smooth transition from the delta function to a broad spectrum, a Lorentzian distribution is used for the phonon spectrum:

$$\alpha^2 F(\omega) = \frac{\lambda'}{\pi}\left(\frac{\delta}{(\omega - \omega_E)^2 + \delta^2} - \frac{\delta}{\eta^2 + \delta^2}\right)\theta(\eta - |\omega_E - \omega|) \tag{3.9}$$

where λ' includes both the normalization of spectrum and the overall strength which is given by:

$$\lambda = 2\int_0^\infty d\omega \frac{\alpha^2 F(\omega)}{\omega}. \tag{3.10}$$

The second part of equation 3.9 is required to ensure that there is no contribution from zero frequency and very high frequencies with no discontinuity in the spectrum. The function is cut both from below and above in order to avoid negativity in the spectrum. The Lorentzian distribution is one of the functions that can be reduced to a delta function with a smooth limiting procedure. For the Lorentzian this limit is taken by letting δ, the width of the Lorentzian, go to zero:

$$\lim_{\delta \longrightarrow 0} \frac{1}{\pi} \frac{\delta}{(\omega - \omega_E)^2 + \delta^2} = \delta(\omega - \omega_E). \tag{3.11}$$

In Figure 3.19, the effect on the density of states due to the electron-phonon interaction is given for different values of the width of the spectrum, δ. As soon as the delta function is broadened, singularities are gone in all places, since the logarithm is integrable. Since the ω_E point is no longer singular, peaks at $n\omega_E$ are smeared out as well. The functional form for the real part of the self-energy is:

$$\begin{aligned} Re\Sigma(\epsilon) = \lambda' \int_0^\infty d\epsilon' N(\epsilon') \Big(& \frac{2(\epsilon + \epsilon' + \omega_E) atan(\frac{\eta}{\delta})}{(\epsilon + \epsilon' + \omega_E)^2 + \delta^2} - \frac{2(-\epsilon + \epsilon' + \omega_E) atan(\frac{\eta}{\delta})}{(-\epsilon + \epsilon' + \omega_E)^2 + \delta^2} \\ & - ln\left|\frac{\eta - \epsilon - \epsilon' - \omega_E}{\eta + \epsilon + \epsilon' + \omega_E}\right| \Big(\frac{\delta}{(\epsilon + \epsilon' + \omega_E)^2 + \delta^2} - \frac{\delta}{\eta^2 + \delta^2} \Big) \\ & + ln\left|\frac{\eta + \epsilon - \epsilon' - \omega_E}{\eta - \epsilon + \epsilon' + \omega_E}\right| \Big(\frac{\delta}{(-\epsilon + \epsilon' + \omega_E)^2 + \delta^2} - \frac{\delta}{\eta^2 + \delta^2} \Big) \Big). \end{aligned} \tag{3.12}$$

For the derivation of this equation, refer to Appendix B. Here, the bare density of states is assumed to be symmetric, and therefore the total density of states is symmetric as well. Although the integrands do not give finite results if integrated one by one, the combination is finite for all energies. As expected in the limit of $\delta \longrightarrow 0$, the results for the Einstein mode are recovered.

Another interesting point is that, energy gets closer to ω_E from below, the structure

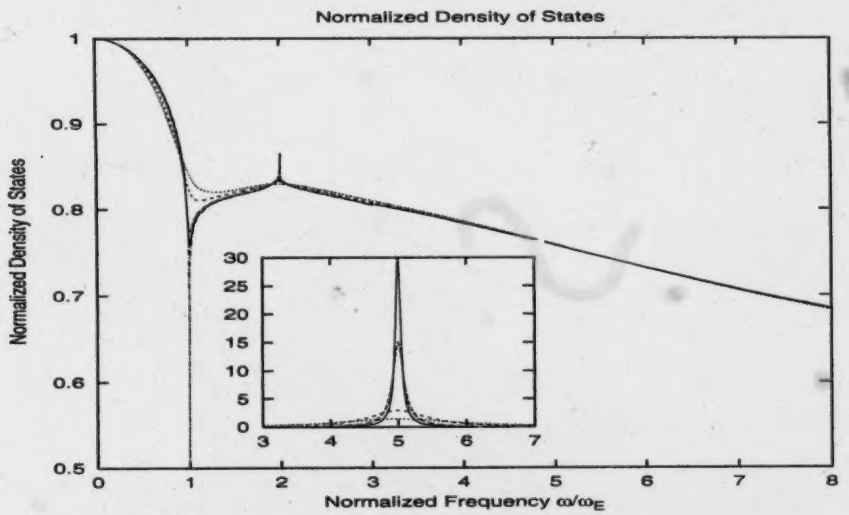

FIGURE 3.19. Modified density of states for $N_s = 1, D/2 = 5\omega_E$ as the width of $\alpha^2 F$ gets wider for a Lorentzian model, shown in inset. δ values are: 0.05 meV(solid line),0.1 meV(long dash),0.5 meV(short dash), 1 meV(dotted),and 0(or Einstein mode)(long dash with dot). Inset shows $\alpha^2 F$ for corresponding non-zero width.

changes as a response to the width of the phonon spectrum. As seen in the equation for the imaginary part of the self-energy, equation 3.8, the limit where the function becomes non-zero decreases with increasing width. Since the non-zero imaginary part reduces the strength of the band, the value of the density of states for that range decreases. However, for values close to ω_E, the singularity dominated for the Einstein mode, and since that is gone, the value of the density of states is increased.

In Figure 3.19, although for many parts of the density of states, the broadening of the phonon spectrum changes the strength of the band, it has almost no effect on the modified bandwidth for this particular choice of variables. However, for

high frequency ($\omega > 10\omega_E$), the enhancement is less with the broad spectrum as expected since less states are lost for low frequencies.

3.6. The center of the phonon spectrum

In the case of an Einstein mode, the energy scale can be reduced to units of Einstein frequency ω_E easily, and therefore the absolute value of the Einstein frequency is not important in the analysis described above. However, in the case of a broad spectrum, the center of the Lorentzian peak might play a role due to the setup of the phonon spectrum. The effect does not show itself explicitly, but rather through the width of the spectrum and the cutoff. The width is chosen to be $\delta = 0.48\omega_E$ to eliminate any sharp effects which are shown in the previous section. As long as η is defined in terms of ω_E, there will be no effect of location of Lorentzian peak in absolute frequencies.

The cutoff parameter, η is chosen to have a lower cutoff in the spectrum close to zero frequency. To give an idea, 3 different center values for the phonon spectrum with same lower cutoff is plotted in Figures 3.20,3.21 and 3.22 for a constant bare density of states and in Figures 3.23, 3.24 and 3.25 for a Lorentzian bare density of states. The difference is barely noticeable, especially between 3.21 and 3.22 and between 3.24 and 3.25, or 5 meV and 15 meV. For a physical phonon spectrum and for computational efficiency for the following parts of the analysis, ω_E=5 meV will be used with a cutoff of η =4.9 meV.

3.7. Effect of Background Band for Broad Phonon Spectrum

The background band is defined to be the effective average band including all other bands, extending from -∞ to +∞ with no frequency dependence. It is the band used in the standard approximation. How this approximation affects the Migdal theory is investigated here, so the effects as the background band gradually

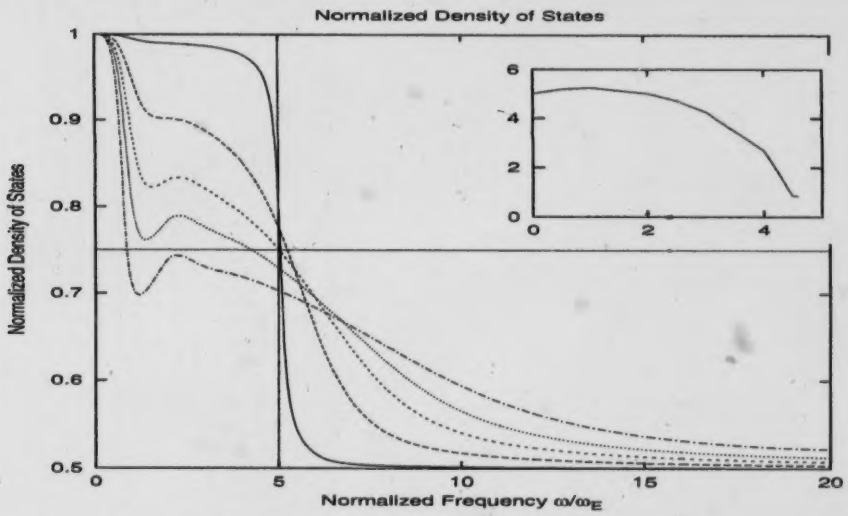

FIGURE 3.20. Modified density of states for $N_s = 1, D/2 = 5\omega_E$ for a Lorentzian phonon distribution at 1meV with constant bare density of states.

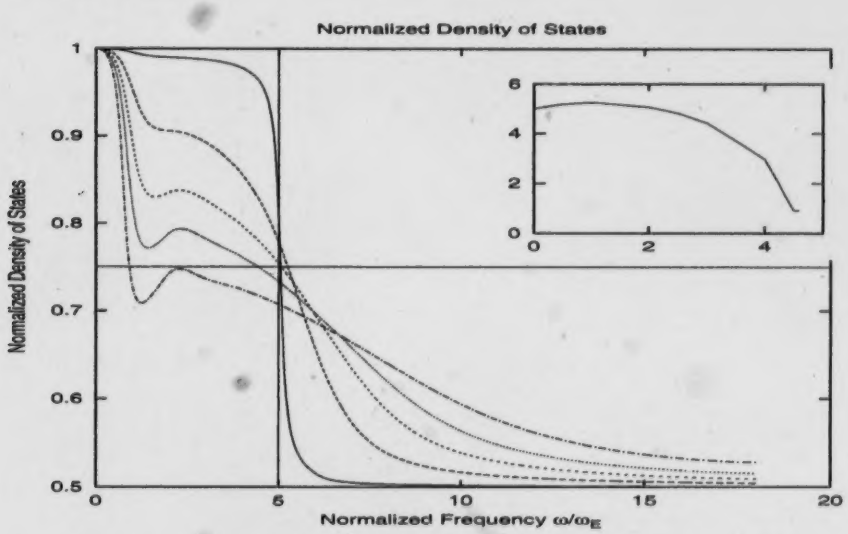

FIGURE 3.21. Modified density of states for $N_s = 1, D/2 = 5\omega_E$ for a Lorentzian phonon distribution at 5meV with constant bare density of states.

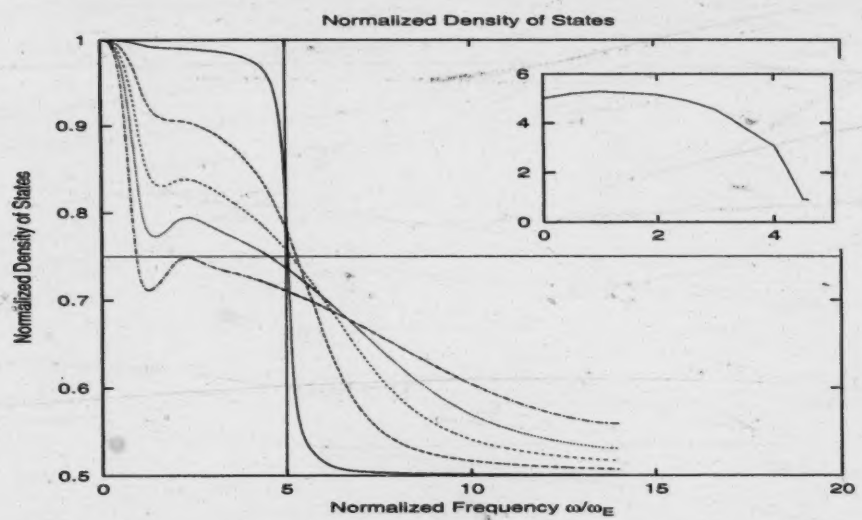

FIGURE 3.22. Modified density of states for $N_s = 1, D/2 = 5\omega_E$ for a Lorentzian phonon distribution at 15meV with constant bare density of states.

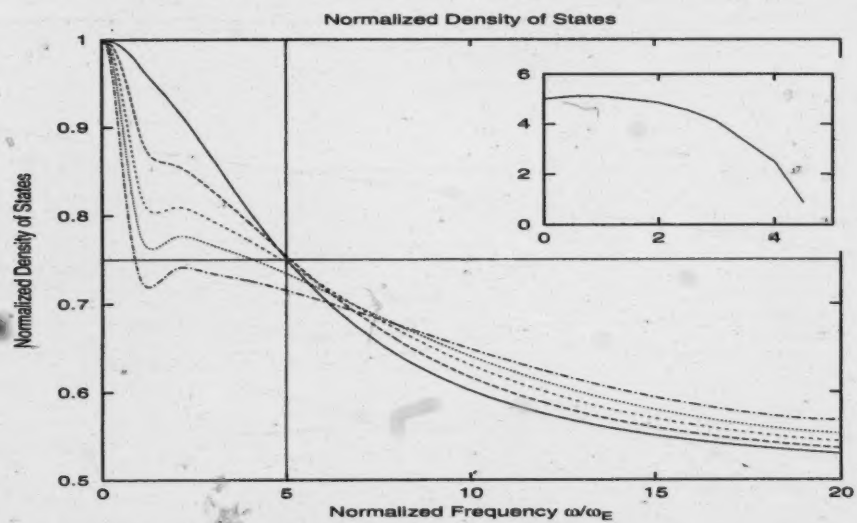

FIGURE 3.23. Modified density of states for $N_s = 1, D/2 = 5\omega_E$ for a Lorentzian phonon distribution at 1meV with Lorentzian bare density of states.

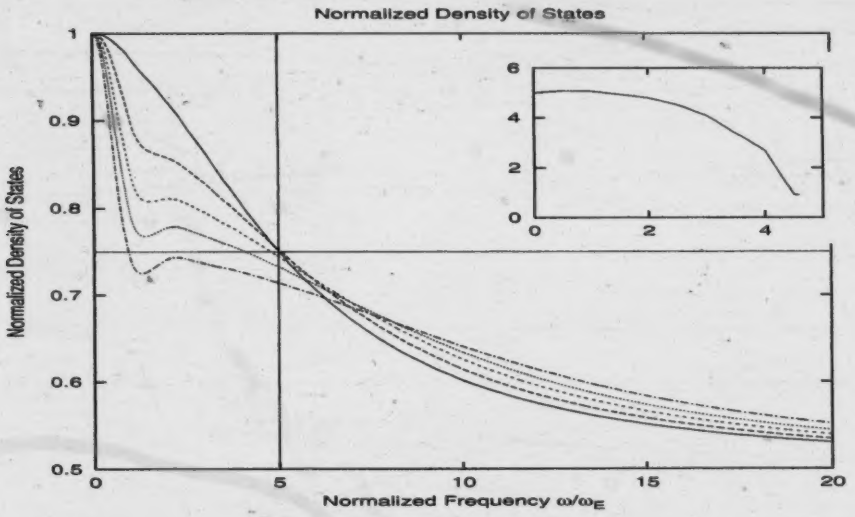

FIGURE 3.24. Modified density of states for $N_s = 1, D/2 = 5\omega_E$ for a Lorentzian phonon distribution at 5meV with Lorentzian bare density of states.

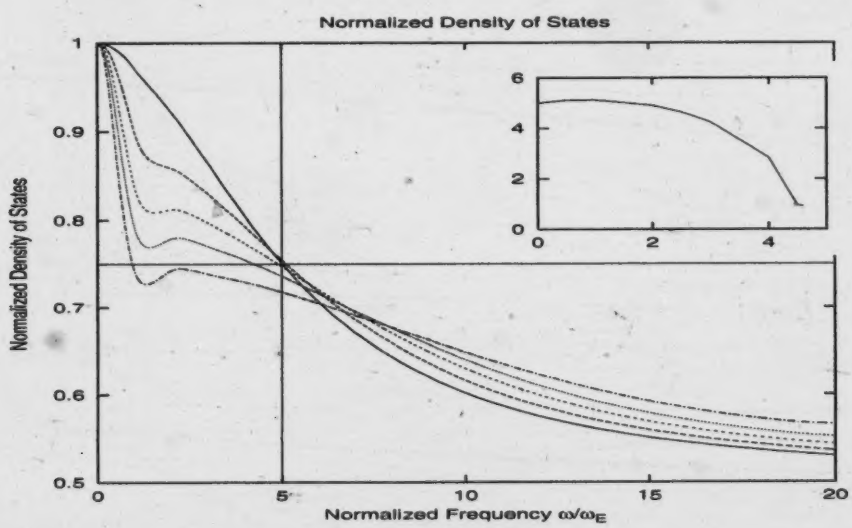

FIGURE 3.25. Modified density of states for $N_s = 1, D/2 = 5\omega_E$ for a Lorentzian phonon distribution at 15meV with Lorentzian bare density of states.

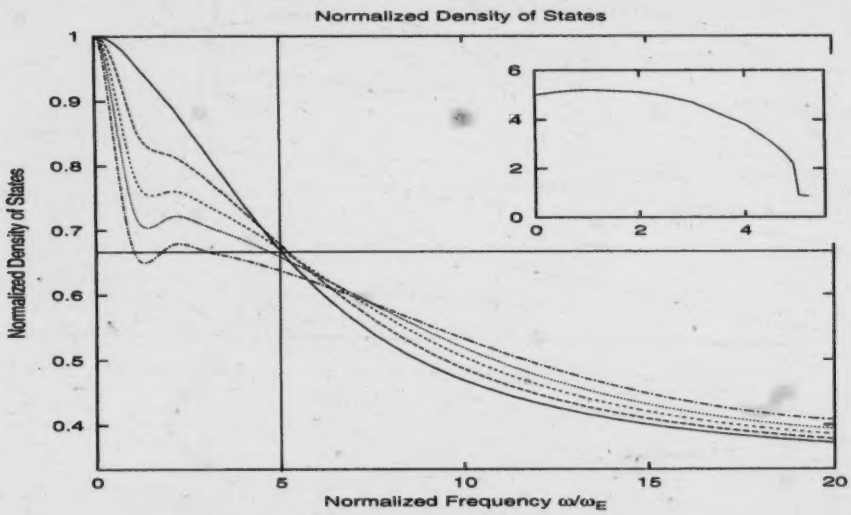

FIGURE 3.26. Modified density of states for $N_s = 0.5, D/2 = 5\omega_E$ for a Lorentzian phonon distribution with Lorentzian bare density of states.

disappears will be investigated. In formula for the density of states, equations 3.2 and 3.5, the background band is denoted by N_s. The analysis for the Einstein mode will be repeated for a phonon spectrum with Lorentzian distribution.

As the weight of the background band decreases, the structure of the affected density of states changes, as shown in Figures 3.24, 3.26 and 3.27 for a Lorentzian bare density of states. The first change to notice is that around ω_E, the depth due to the electron phonon peak decreases as background band is reduced. However the peak at $2\omega_E$, due to the minimum at ω_E, becomes sharper. Consequently, a minimum starts to form near $3\omega_E$. However, since the $2\omega_E$ peak is not strong, the $3\omega_E$ feature does not appear as a minimum, but rather as a slight decrease. The extra states at high frequency occurring due to the suppression of low energy states mainly occurs around 5-10ω_E. The very high frequency part is enhanced less with decreasing background. Examples are shown in Figures 3.26 and 3.27. In addition to these changes, the dependence of the modified bandwidth on the electron phonon

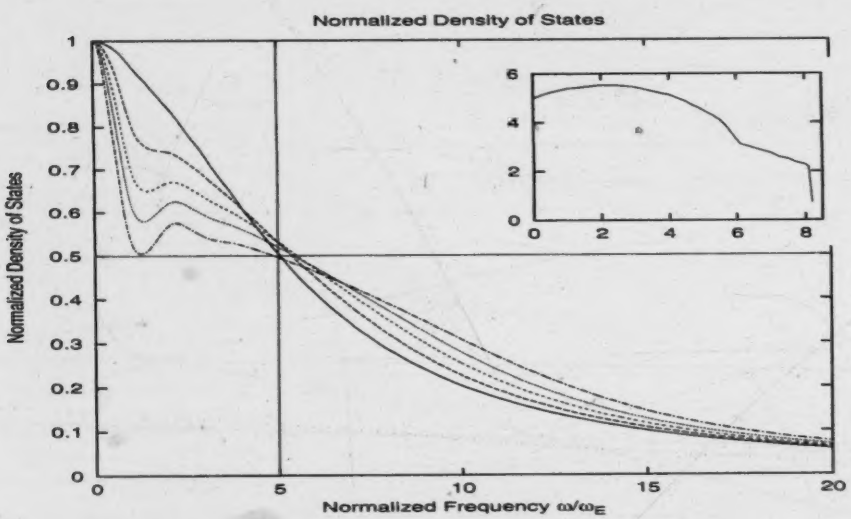

FIGURE 3.27. Modified density of states for $N_s = 0, D/2 = 5\omega_E$ for a Lorentzian phonon distribution with Lorentzian bare density of states.

interaction dependence is modified as well. To start with, the range that the bandwidth is not reduced due to electron-phonon interaction strength is almost doubled. Additional features are present due to $n\omega_E$ structures in the density of states. The peak at $2\omega_E$ causes the dependence of the modified bandwidth on the electron-phonon strength to jump from $2\omega_E$ to less than ω_E, as shown in Figures 3.26 and 3.27

In the case of constant bare density of states, the features described becomes more apparent, as shown in Figures 3.21, 3.28 and 3.29. In the case where $N_s = 1$, even for very small λ, contrary to the Lorentzian case, the reduction due to the electron-phonon interaction is noticeable. To compensate the loss of states at low energy, enhancement at higher energies is observed. For even very small electron-phonon strength, the tail extends to $10\omega_E$. Since the bare density of states has no contribution from outside the bandwidth, any contribution in this frequency range is important. For higher strengths, the tail extends to much higher frequencies,

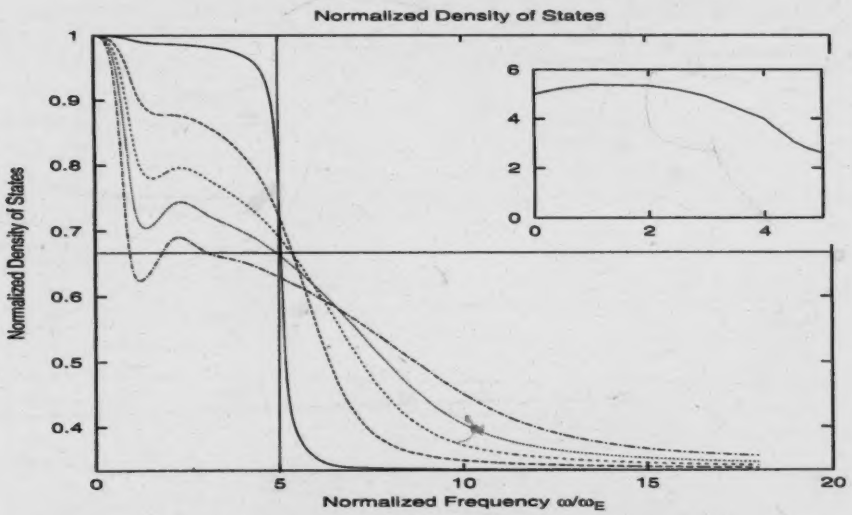

FIGURE 3.28. Modified density of states for $N_s = 0.5, D/2 = 5\omega_E$ for a Lorentzian phonon distribution with constant bare density of states.

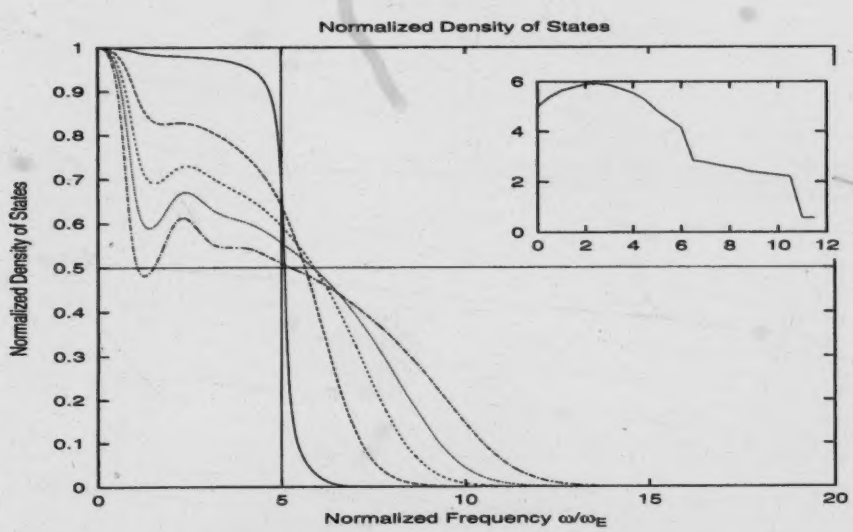

FIGURE 3.29. Modified density of states for $N_s = 0, D/2 = 5\omega_E$ for a Lorentzian phonon distribution with constant bare density of states.

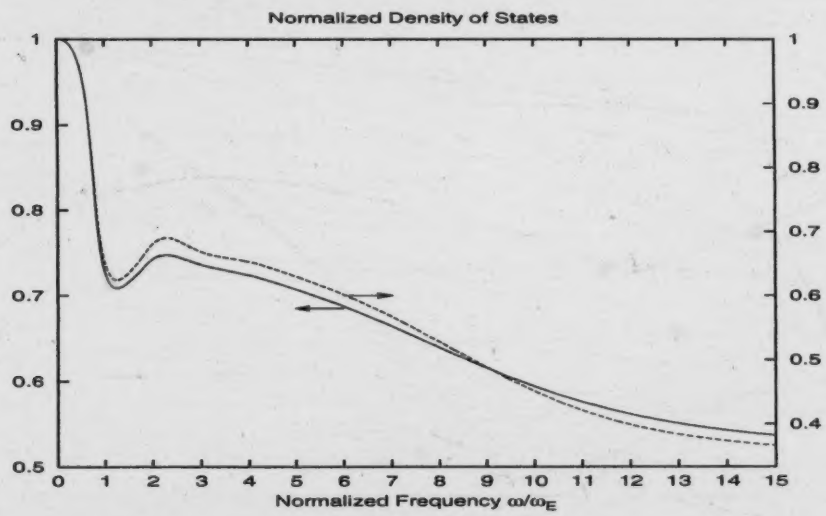

FIGURE 3.30. Modified density of states for $N_s = 1$(solid) and $N_s = 0.5$(dashed) $D/2 = 5\omega_E$ for a Lorentzian phonon distribution with constant bare density of states.

effectively increasing the absolute bandwidth. Here, the effect of background band is clear. Although the background band is not frequency dependant and extends to infinity, its very existence affects the outcome of the electron-phonon coupling with a band with finite bandwidth. When the background influence is reduced to a third of the total states, the high energy tail is less enhanced for the same electron-phonon strength, and when the background band is eliminated altogether, the enhancement goes up to only $7\omega_E$. The overall shift occurs at frequencies between approximately $5\omega_E$ and $10\omega_E$. To show this change, the density of states for $N_s = 1$ and $N_s = 0.5$ is plotted in Figure 3.30 and $N_s = 0.5$ and $N_s = 0$ is plotted in Figure 3.31, all for $\lambda = 4.5$. It is important to note that the complete bandwidth is extended for higher electron-phonon strength. The extension is not in the form of merely a tail, but rather as a part of a frequency dependant band, especially in the case without a background band. The strength of the enhanced

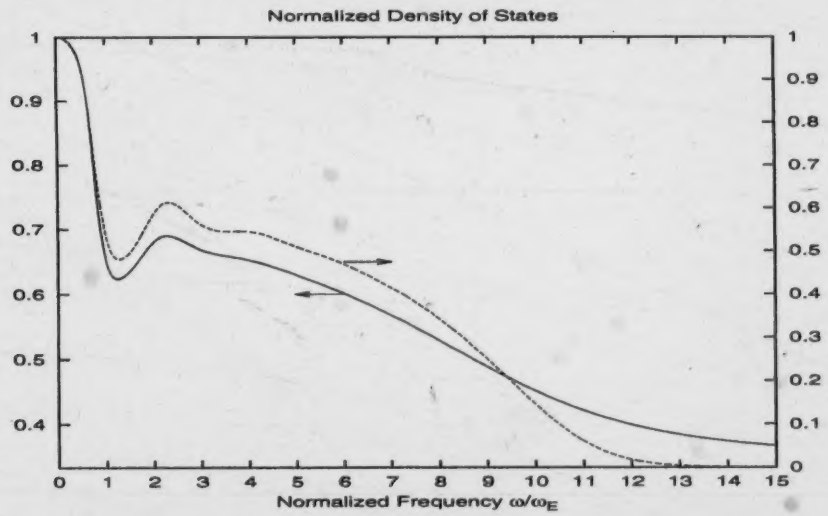

FIGURE 3.31. Modified density of states for $N_s = 0.5$(solid) and $N_s = 0$(dashed) $D/2 = 5\omega_E$ for a Lorentzian phonon distribution with constant bare density of states.

part is almost the same as the modified strength of the density of states within the range of the bare bandwidth ($5\omega_E$).

3.8. Effect of the Bare Bandwidth Value for Broad Phonon Spectrum

In this section, the effect of having a bare bandwidth with $D = 20\omega_E$ instead of $10\omega_E$ is investigated for different background band strengths. When the background band has equal strength at Fermi level to the band of interest, for a Lorentzian bare density of states, a mostly uniform effect on the density of states is observed for intermediate values of λ as shown in Figure 3.32. Since electrons around ω_E are affected through single phonon processes, most of the suppression is focused in that region. However, a non-zero self-energy affects other energy ranges as well. The states lost due to the electron-phonon coupling are compensated by an enhancement at higher energies. In Figure 3.32, an important point to note is that enhancement extends for very large energies compared to the characteristic

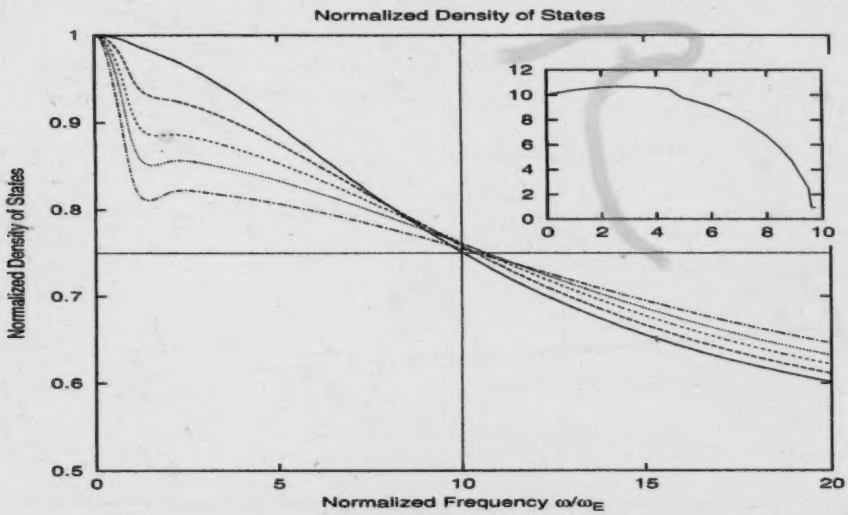

FIGURE 3.32. Modified density of states for $N_s = 1, D/2 = 10\omega_E$ for a Lorentzian phonon distribution with Lorentzian bare density of states.

phonon frequency. The enhancement is proportional to the bare bandwidth when it is compared to the same set of variables with bandwidth reduced to half. In other words, the structure is identical in both shape and size if frequencies up to $10\omega_E$ with $10\omega_E$ bandwidth is compared to frequencies up to $20\omega_E$ with $20\omega_E$ bandwidth. Low frequencies are not comparable since for both cases the phonon frequency is at ω_E. The trend is the same in both cases around ω_E, as expected. As the background band is reduced with respect to the band of interest, the high energy enhancement occurs at energies close to the bare bandwidth energies (10-$20\omega_E$) as shown in Figures 3.33 and 3.34 as in the case of $10\omega_E$ in Figures 3.26 and 3.27. The feature at ω_E is more apparent for smaller background bands. As a result, the $n\omega_E$ structures begin to form.

The case of constant bare density of states is consistent with the observations above. This case shows better that the existence of a background band extends the range of finite band well beyond the original cutoff. For the case $N_s = 1$,

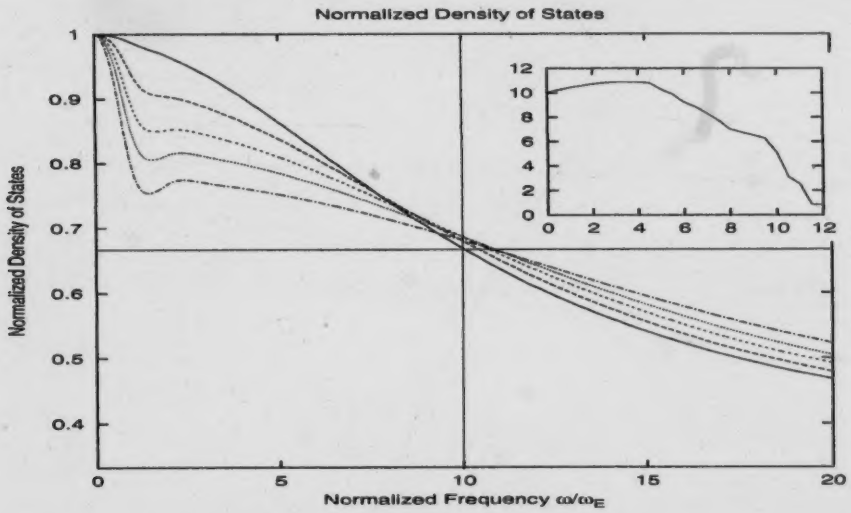

FIGURE 3.33. Modified density of states for $N_s = 0.5, D/2 = 10\omega_E$ for a Lorentzian phonon distribution with Lorentzian bare density of states.

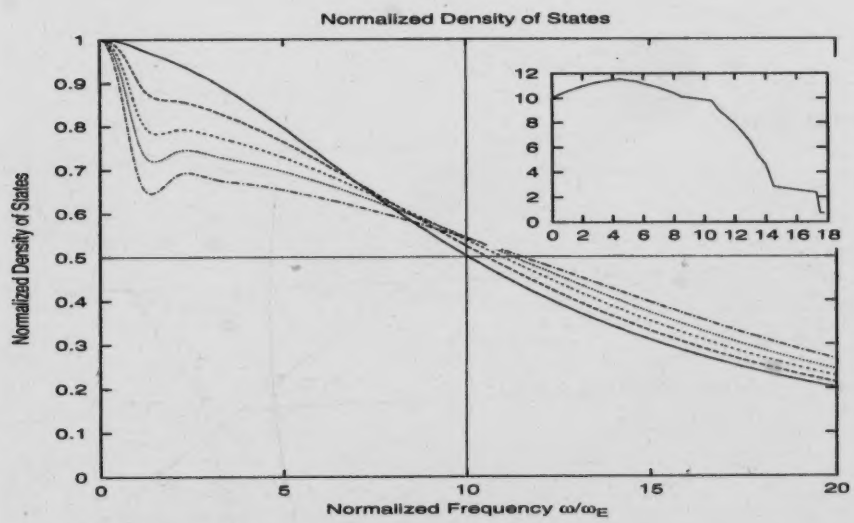

FIGURE 3.34. Modified density of states for $N_s = 0, D/2 = 10\omega_E$ for a Lorentzian phonon distribution with Lorentzian bare density of states.

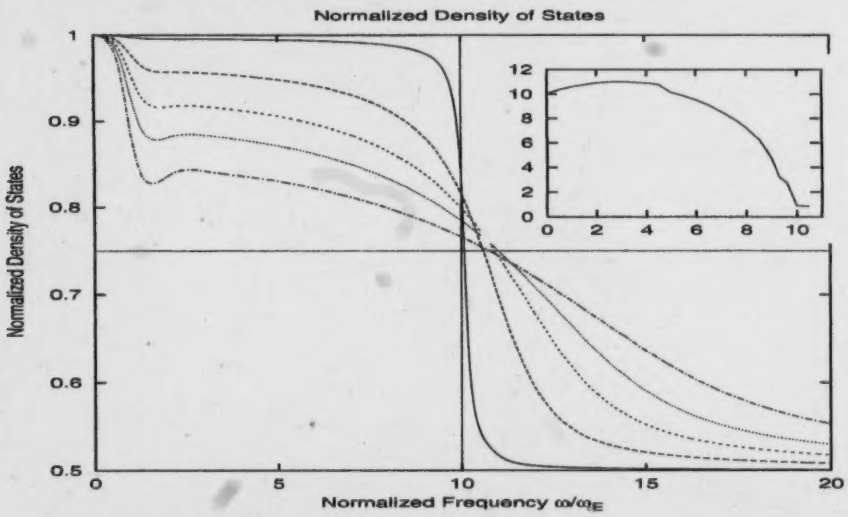

FIGURE 3.35. Modified density of states for $N_s = 1, D/2 = 10\omega_E$ for a Lorentzian phonon distribution with constant bare density of states.

the range that the finite band has a large contribution, and extends from $10\omega_E$ to over $20\omega_E$ when the electron-phonon interaction strength reaches $\lambda = 4.5$, as shown in Figure 3.35. When the background is removed, the extension is reduced significantly. The remaining extension is no longer merely a tail but a significant part of the band which extends beyond $15\omega_E$ as shown in Figures 3.36 and 3.37.

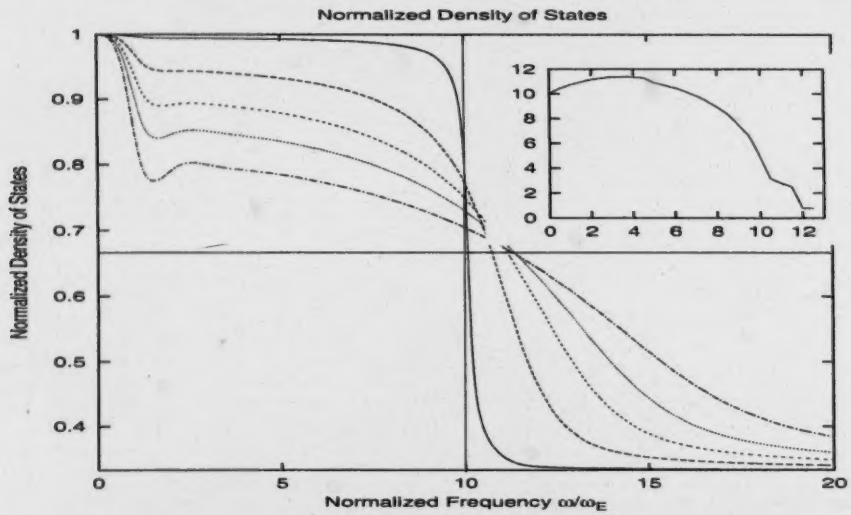

FIGURE 3.36. Modified density of states for $N_s = 0.5, D/2 = 10\omega_E$ for a Lorentzian phonon distribution with constant bare density of states.

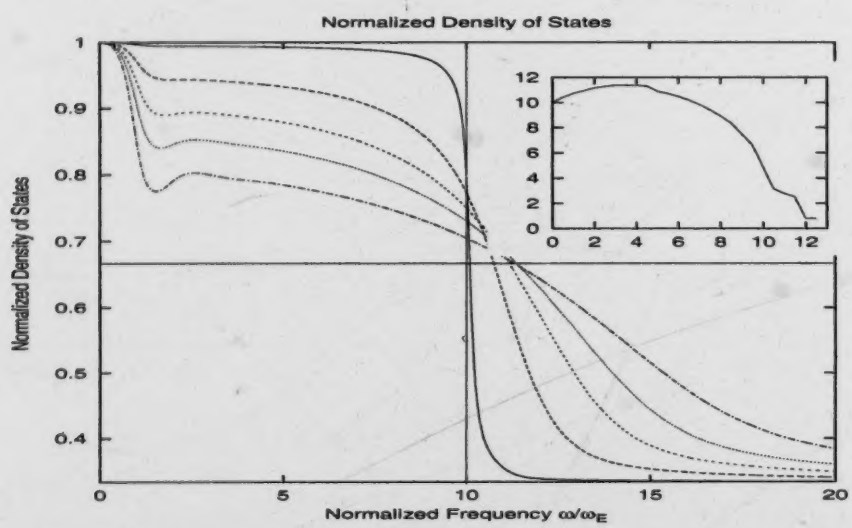

FIGURE 3.37. Modified density of states for $N_s = 0.5, D/2 = 10\omega_E$ for a Lorentzian phonon distribution with constant bare density of states.

CHAPTER 4

Conclusions

In this thesis, some assumptions of Migdal's theory have been questioned. The assumption that the density of states can be written as a constant and an infinite range has been relaxed, along with the use of the non-interacting electron Green function in the self-energy. It is shown that the use of the full Green function without a frequency dependant density of states gives no modification to both the density of states and the self-energy. In order to see the effect of a frequency dependant density of states on the self-energy self-consistently, one must use the full Green function; otherwise, effects are not observed completely.

One of the earlier works[**16**] has been improved by carrying the derivation forward analytically. This enabled the artifacts due to the use of the Einstein mode to be made explicit analytically. For even very small interaction strength, a singularity in the formalism causes the band to collapse. In return, due to the fact that the self-energy at intervals of the characteristic phonon frequency are related, multiple-phonon processes modify the density of states at $n\omega_E$. Although this relation holds for an arbitrary electron-phonon spectral function, the nature of the Einstein mode causes the effects to be extreme. When the electron-phonon spectral function is replaced by a more realistic one, a Lorentzian distribution, all such singularities are removed. Although the effects did not disappear completely, the effects on the density of states and the self-energy have been reduced. In other words, the main contribution of this change was the fact that the singularity has been removed, and a more realistic effect has been observed with a minimum near ω_E.

In order to differentiate the effect of a narrowed band from additional frequency

dependence, two different bare densities of states are implemented. The first one, which was used by Alexandrov et al[**16**], was a Lorentzian. This function is non-zero for a very long range of frequencies, and can be considered as a function which extends to very high frequencies; therefore for one part of the analysis, a more compact function is required. The other model function used is the constant bare density of states with the same bandwidth as the Lorentzian. Since the function is more compact, effects of having a finite range of frequencies for the density of states are more visible with the same set of parameters as the Lorentzian. Due to this same reason, many artifacts of the Einstein mode are revealed more clearly. Another question that was addressed in this thesis is: how does the existence of a second background band influence the results obtained so far?

As the weight of the frequency dependent band becomes dominant, although it requires higher λ to get the same effect, the overall effect on the total density of states becomes more enhanced. This enhancement is especially evident for an Einstein mode. As the background band disappears, the value of the density of states drops to zero and at the singularity, the band disappears. Due to this feature, multiple-phonon processes affect the density of states at $n\omega_E$ drastically.

Another important result of this analysis is the enhancement to the modified bandwidth observed at intermediate values of λ. The enhancement gets larger as the bandwidth gets larger or as the background band disappears. This shows that, although the electron-phonon interaction reduces the density of states around the characteristic phonon frequency, it actually increases the overall bandwidth. This is consistent with the constraint that the density of states obeys a sum rule, and states lost at energies close to the Fermi level must move to higher frequencies. This shift can extend the band to twice its original width.

Here, extreme cases have been investigated. In normal conditions, it is not common to have a band at the Fermi surface of a real metal which contributes half of the

states and has such a short bandwidth, in this case of the order of 10-20 times the phonon frequency. The author wants to emphasize the effect of a finite bandwidth. It is one of the reasons for the use of this short bandwidth; the other is that although the characteristic phonon frequency used in this calculation is 5 meV, since all calculations were carried out for normalized frequencies, for phonon frequencies of the order of 50 meV, the analysis above holds for a bandwidth of around 1 eV, which is a very large affected range. In general, particle-hole symmetry does not hold for metals. Although the density of states at the Fermi level does not change in this case, in general the Fermi level can change with electron-phonon interaction, causing the density of states at the Fermi level to change. In order to understand the different width of bands, two distinct cases are investigated here, and it is seen that as the bandwidth gets larger, the modification due to the electron-phonon interaction on the density of states becomes less effective. This result is consistent with the assumption that in the constant density of states with infinite bandwidth the electron-phonon interaction does not modify the density of states.

In the future, the case with no particle-hole symmetry could be analyzed. Changes to the density of states at the Fermi level could be investigated. A more realistic density of states can be used as the bare one. The approximation that no vertex correction is required would be investigated. For the phonon spectrum, instead of a theoretical distribution, experimental input could be used, although this should result in little qualitative change.

Bibliography

[1] Grimvall, G. *The Electron-phonon interaction in Metals*Netherlands: North Holland Publishing Co. 1981.

[2] Ashcroft, N.W. and N.D. Mermin, *Solid State Physics* PA:Saunders Collage.

[3] Grimvall, G. Physica Scripta 12(1975)337.

[4] Lanzara A, P.V. Bogdanov,X.J. Zhou,S.A. Kellar, D.L. Feng, E.D. Lu,T. Yoshida,H. Eisaki, A. Fujimori,K.Kishio, J.I. Shimoyama,T.Noda, S. Uchida, Z. Hussain and Z.X Shen. Nature 412(2001)510.

[5] Verga S., A. Knigavko, F. Marsiglio, cond-mat/0207145.

[6] Bardeen, J., L.N. Cooper, J.R. Schrieffer, F., Physical Rev. 108(1957)1175.

[7] Eliashberg, G.M., JETP 37(1960)261.

[8] Parks, R.D., *Superconductivity*,(Marcel Dekker Inc, New York, 1969).

[9] Marsiglio,F., J. Carbotte, cond-mat/0106143, to Review Chapter to appear in 'The Physics of Conventional and Unconventional Superconductors' edited by K.H. Bennemann and J.B. Ketterson (Springer-Verlag)

[10] Landau, L. D., Phys. Z.Sowjetunion 3(1933)664.

[11] Alexandrov, A.S., Sir Nevill Mott, *Polarons and Bipolarons* Singapore: World Scientific 1995

[12] Marsiglio, F., Physica C 244(1995)21.

[13] Migdal, A.B., JETP 34(7)(1958)996.

[14] Nakajima, S., Y. Toyozawa, R. Abe, *The Physics of Elementary Excitations* New York: Springer-Verlag 1980.

[15] Engelsberg, S., J.R. Schrieffer, Physical Rev 131(1963)993.

[16] Alexandrov, A.S., V.N Grebenev, E.A. Mazur, JETP 45(1987)455.

[17] Holstein, T., Ann. Phys.(New York) 8(1959)325.

[18] Marsiglio, F., Phys. Rev. B 42(1990)2416.

[19] Mahan,G.D., *Many Particle Physics* New York: Kluwer Academic/Plenum Publishers 2000.

[20] P.B. Allen and B. Mitrović, in *Solid State Physics*, edited by H. Ehrenreich, F. Seitz, and D. Turnbull (Academic, New York, 1982) Vol. 37, p.1.

[21] Baym G., D Mermin, J. Math. Phys. 2(1961)232.

[22] The equation for the density of states (Eq.3.2) is solved numerically using the real and the imaginary parts of the self-energy (Eq.3.1 and Eq.3.3 respectively) with self-consistent iterations. The singularity is handled analytically as shown in Appendix B. For the convergence condition, average variance of the normalized density of states is calculated and when it is less than 1×10^{-4}, iteration is concluded. For different bare densities of states and different electron-phonon coupling strengths respective equations are used with same condition. The convergence is slower with increasing λ since multiple-phonon effects are more observable with increasing λ. The choice of bare density of states does not affect convergence but with strong background band, convergence is faster since the electron-phonon interaction affects less with background band. Using a solution with smaller λ with same parameters as input helps convergence since in that solution most of the multi-phonon effects are included. The cutoff energy is six times the bare bandwidth to take into account all the enhancements in high energies.

APPENDIX A

Derivation of Density of States Equation for Specific Distributions

As shown in section 2, the modified density of states in context of Green function is given by the equation:

$$N(\epsilon) = \int_{-\infty}^{\infty} d\xi N_0(\xi) A(\xi, \epsilon), \tag{A.1}$$

which is equivalent to:

$$N(\epsilon) = -\frac{1}{\pi} \int_{-\infty}^{\infty} d\xi N_0(\xi) ImG(\xi, \epsilon), \tag{A.2}$$

where

$$G^{-1}(\xi, \epsilon) = \epsilon - \xi - \Sigma(\epsilon) \tag{A.3}$$

and

$$A(\xi, \epsilon) = -\frac{1}{\pi} ImG(\xi, \epsilon). \tag{A.4}$$

Here, using different bare density of state functions, how the complete density of state functions are reached will be discussed.

A.1. Lorentzian Bare Density of States

Here, the bare density of states is described by a Lorentzian which has width of D/2 centered around Fermi Energy, set to zero. The functional form of the density of states, including a background band, is:

$$N_0(\xi) = \frac{1}{1 + N_s} [\frac{D^2/4}{\xi^2 + D^2/4} + N_s]. \tag{A.5}$$

Therefore, for this case, the total density of states is:

$$N(\epsilon) = -\frac{1}{\pi}\frac{1}{1+N_s}\int_{-\infty}^{\infty} d\xi[\frac{D^2/4}{\xi^2+D^2/4} + N_s]ImG(\xi,\epsilon). \tag{A.6}$$

or,

$$N(\epsilon) = \frac{1}{\pi}\frac{1}{1+N_s}\int_{-\infty}^{\infty} d\epsilon'[\frac{D^2/4}{\epsilon'^2+D^2/4}+N_s]\frac{|Im\Sigma(\epsilon)|}{(\epsilon-\epsilon'-Re\Sigma(\epsilon))^2+|Im\Sigma(\epsilon)|^2}. \tag{A.7}$$

Separating the integral, one obtains:

$$N(\epsilon) = \frac{1}{\pi}\frac{1}{1+N_s}[\int_{-\infty}^{\infty} d\epsilon'\frac{D^2/4}{\epsilon'^2+D^2/4}(\frac{|Im\Sigma(\epsilon)|}{(\epsilon-\epsilon'-Re\Sigma(\epsilon))^2+|Im\Sigma(\epsilon)|^2}) + N_s\int_{-\infty}^{\infty} d\epsilon'(\frac{|Im\Sigma(\epsilon)|}{(\epsilon-\epsilon'-Re\Sigma(\epsilon))^2+|Im\Sigma(\epsilon)|^2})]. \tag{A.8}$$

The second integrand is the imaginary part of the Green function, or electron spectral function upto a factor of π. Since the spectral function is normalized, the integral is π. The first part is:

$$|Im\Sigma(\epsilon)|D^2/4[\frac{1}{D/2((iD/2-\epsilon+Re\Sigma(\epsilon))^2+|Im\Sigma(\epsilon)|^2)} + \frac{1}{|Im\Sigma(\epsilon)|((i|Im\Sigma(\epsilon)|+\epsilon-Re\Sigma(\epsilon))^2+D^2/4)}], \tag{A.9}$$

which can be reduced to the form:

$$\frac{D/2(D/2+|Im\Sigma(\epsilon)|)}{(Re\Sigma(\epsilon)-\epsilon)^2+(|Im\Sigma(\epsilon)|+D/2)^2} \tag{A.10}$$

by a straightforward calculation. Therefore:

$$N(\epsilon) = \frac{1}{1+N_s}(\frac{D/2(D/2+|Im\Sigma(\epsilon)|)}{(Re\Sigma(\epsilon)-\epsilon)^2+(|Im\Sigma(\epsilon)|+D/2)^2}+N_s). \tag{A.11}$$

A.2. Constant Bare Density of States

In this case, the bare density of states is described by a constant function with finite width in addition to another band with infinite bandwidth. The functional form of the density of states is:

$$N_0(\epsilon) = \frac{1}{1+N_s}[\theta(\omega_c - |\epsilon|) + N_s] \tag{A.12}$$

where $\theta(x)$ is the Heaviside step function defined as:

$$\theta(x) = \begin{cases} 0;\ x < 0 \\ 1;\ x > 0 \end{cases} \tag{A.13}$$

The modification to the total density of states is:

$$N(\epsilon) = -\frac{1}{\pi}\frac{1}{1+N_s}\int_{-\infty}^{\infty} d\xi[\theta(\omega_c - |\xi|) + N_s]ImG(\xi,\epsilon), \tag{A.14}$$

or,

$$N(\epsilon) = \frac{1}{\pi}\frac{1}{1+N_s}\int_{-\infty}^{\infty} d\epsilon'[\theta(\omega_c - |\epsilon'|) + N_s](\frac{|Im\Sigma(\epsilon)|}{(\epsilon - \epsilon' - Re\Sigma(\epsilon))^2 + |Im\Sigma(\epsilon)|^2}. \tag{A.15}$$

The part with constant background is the same as the Lorentzian. The step function modifies the integral to:

$$N(\epsilon) = \frac{1}{\pi}\frac{1}{1+N_s}[\int_{-\omega_c}^{\omega_c} \frac{|Im\Sigma(\epsilon)|d\epsilon'}{(\epsilon - \epsilon' - Re\Sigma(\epsilon))^2 + |Im\Sigma(\epsilon)|^2} + \pi N_s], \tag{A.16}$$

resulting in:

$$N(\epsilon) = \frac{1}{\pi}\frac{1}{1+N_s}(\arctan(\frac{Re\Sigma(\epsilon) + \omega_c - \epsilon}{|Im\Sigma(\epsilon)|}) - \arctan(\frac{Re\Sigma(\epsilon) - \omega_c - \epsilon}{|Im\Sigma(\epsilon)|}) + \pi N_s). \tag{A.17}$$

APPENDIX B

Derivation of Electron Self-Energy for Specific Phonon Spectrum

In this section, the derivation of the real part of the self-energy for several cases will be discussed. As shown in section 2, the self-energy of the electron in a general form is:

$$\Sigma(\omega+i\delta) = \int_{-\infty}^{\infty} d\epsilon' N(\epsilon') \int_0^{\infty} d\Omega \alpha^2 F(\Omega)[\frac{n(\Omega)+f(-\epsilon')}{\omega+i\delta-\Omega-\epsilon'}+\frac{n(\Omega)+f(\epsilon')}{\omega+i\delta+\Omega-\epsilon'}]. \tag{B.1}$$

From this equation, the real and imaginary parts of the self-energy can be derived as:

$$Re\Sigma(\omega) = \int_{-\infty}^{\infty} d\epsilon' N(\epsilon') \int_0^{\infty} d\Omega \alpha^2 F(\Omega)[\frac{n(\Omega)+f(-\epsilon')}{\omega-\Omega-\epsilon'} + \frac{n(\Omega)+f(\epsilon')}{\omega+\Omega-\epsilon'}] \tag{B.2}$$

and

$$Im\Sigma(\omega) = -\pi \int_0^{\infty} d\Omega \alpha^2 F(\Omega)[N(\omega-\Omega)(n(\Omega)+f(\Omega-\omega))+N(\omega+\Omega)(n(\Omega)+f(\Omega+\omega))]. \tag{B.3}$$

Here, zero temperature conditions are investigated. The Bose function, $n(\omega)$, is zero and the Fermi function, $f(\omega)$, is a step function at zero temperature. The equations become:

$$Re\Sigma(\omega) = \int_{-\infty}^{\infty} d\epsilon' N(\epsilon') \int_0^{\infty} d\Omega \alpha^2 F(\Omega)[\frac{\theta(\epsilon')}{\omega-\Omega-\epsilon'} + \frac{\theta(-\epsilon')}{\omega+\Omega-\epsilon'}] \tag{B.4}$$

and

$$Im\Sigma(\omega) = -\pi \int_0^\infty d\Omega \alpha^2 F(\Omega)[N(\omega-\Omega)\theta(\omega-\Omega)+N(\omega+\Omega)(1-\theta(\Omega+\omega))]. \tag{B.5}$$

B.1. Einstein Mode

For the Einstein mode, the phonon spectrum, $\alpha^2 F(\Omega)$ is defined by a delta function:

$$\alpha^2 F(\Omega) = \frac{\lambda \omega_E}{2} \delta(\Omega - \omega_E) \tag{B.6}$$

The delta function allows the Ω-integral in equations B.4 and B.5 to be readily performed:

$$Re\Sigma(\omega) = \frac{\lambda \omega_E}{2} \int_{-\infty}^{\infty} d\epsilon' N(\epsilon')[\frac{\theta(\epsilon')}{\omega - \omega_E - \epsilon'} + \frac{\theta(-\epsilon')}{\omega + \omega_E - \epsilon'}] \tag{B.7}$$

and

$$Im\Sigma(\omega) = -\frac{\lambda \omega_E \pi}{2}[N(\omega-\omega_E)\theta(\omega-\omega_E)+N(\omega+\omega_E)(1-\theta(\omega_E+\omega))]. \tag{B.8}$$

At this point, the imaginary part is found for the given spectrum. The real part is not yet complete. First, the integral is separated into 2 parts to eliminate the step functions:

$$Re\Sigma(\omega) = \frac{\lambda \omega_E}{2} \int_0^\infty \frac{d\epsilon' N(\epsilon')}{\omega - \omega_E - \epsilon'} + \int_{-\infty}^0 \frac{d\epsilon' N(\epsilon')}{\omega + \omega_E - \epsilon'}. \tag{B.9}$$

Using the assumption that the density of states is symmetric, the integrals can be combined:

$$Re\Sigma(\omega) = \frac{\lambda \omega_E}{2} \int_0^\infty d\epsilon' N(\epsilon')[\frac{1}{\omega - \omega_E - \epsilon'} + \frac{1}{\omega + \omega_E + \epsilon'}]. \tag{B.10}$$

The integrands are singular within the integral range. Most of the singularities that appear in equation B.10 are cancelled because for any positive infinity, there is a negative one, making the final result finite. However, for self-energy at ω_E, same

conclusion cannot be made. In equation B.10, denominator becomes singular at origin. To understand if the singularity survives after the integration, the integral is separated into two parts, the well-behaved part and the possibly singular part:

$$Re\Sigma(\omega) = \frac{\lambda\omega_E}{2}\int_0^\infty d\epsilon'[(N(\epsilon') - N(\omega-\omega_E))[\frac{1}{\omega-\omega_E-\epsilon'} + \frac{1}{\omega+\omega_E+\epsilon'}] + N(\omega-\omega_E)[\frac{1}{\omega-\omega_E-\epsilon'} + \frac{1}{\omega+\omega_E+\epsilon'}]] \quad \text{(B.11)}$$

The first part is now finite for all energies, since the numerator is zero where the denominator is. All singularities are included in second part:

$$Re\Sigma(\omega) = \frac{\lambda\omega_E}{2}[\int_0^\infty d\epsilon' \frac{2\epsilon'(N(\epsilon') - N(\omega-\omega_E))}{\omega^2 - (\omega_E+\epsilon')^2} + N(\omega-\omega_E) ln|\frac{\omega-\omega_E}{\omega+\omega_E}|]. \quad \text{(B.12)}$$

B.2. Lorentzian Spectrum

In this section, the same derivation will be repeated for the Lorentzian phonon spectrum. The spectrum to be used is:

$$\alpha^2F(\Omega) = \frac{\lambda'}{\pi}(\frac{\delta}{(\Omega-\omega_E)^2+\delta^2} - \frac{\delta}{\eta^2+\delta^2})\theta(\eta - |\omega_E - \Omega|). \quad \text{(B.13)}$$

Starting from equation B.4,

$$Re\Sigma(\omega) = \int_0^\infty d\epsilon' N(\epsilon')[\int_0^\infty d\Omega\alpha^2F(\Omega)(\frac{1}{\omega-\Omega-\epsilon'} + \frac{1}{\omega+\Omega+\epsilon'})], \quad \text{(B.14)}$$

using the spectrum given above:

$$Re\Sigma(\omega) = \int_0^\infty d\epsilon' N(\epsilon')[\int_0^\infty d\Omega\frac{\lambda'}{\pi}(\frac{\delta}{(\Omega-\omega_E)^2+\delta^2} - \frac{\delta}{\eta^2+\delta^2})\theta(\eta - |\omega_E-\Omega|) \times(\frac{1}{\omega-\Omega-\epsilon'} + \frac{1}{\omega+\Omega+\epsilon'})] \quad \text{(B.15)}$$

or:

$$Re\Sigma(\omega) = \int_0^\infty d\epsilon' N(\epsilon')[\int_{\omega_E-\eta}^{\omega_E+\eta} d\Omega \frac{\lambda'}{\pi}(\frac{\delta}{(\Omega-\omega_E)^2+\delta^2} - \frac{\delta}{\eta^2+\delta^2}) \times(\frac{1}{\omega-\Omega-\epsilon'} + \frac{1}{\omega+\Omega+\epsilon'})]. \quad \text{(B.16)}$$

Separating the integral into two parts, one obtains:

$$Re\Sigma(\omega) = \int_0^\infty d\epsilon' N(\epsilon')[\int_{\omega_E-\eta}^{\omega_E+\eta} d\Omega \frac{\lambda'}{\pi}(\frac{\delta}{(\Omega-\omega_E)^2+\delta^2}(\frac{1}{\omega-\Omega-\epsilon'} + \frac{1}{\omega+\Omega+\epsilon'}) - \frac{\delta}{\eta^2+\delta^2}(\frac{1}{\omega-\Omega-\epsilon'} + \frac{1}{\omega+\Omega+\epsilon'})) \quad \text{(B.17)}$$

The second part gives a logarithm, whereas the first part gives arctangent with logarithm. The result is:

$$Re\Sigma(\epsilon) = \lambda' \int_0^\infty d\epsilon' N(\epsilon')(\frac{2(\epsilon+\epsilon'+\omega_E)atan(\frac{\eta}{\delta})}{(\epsilon+\epsilon'+\omega_E)^2+\delta^2} - \frac{2(-\epsilon+\epsilon'+\omega_E)atan(\frac{\eta}{\delta})}{(-\epsilon+\epsilon'+\omega_E)^2+\delta^2} - ln|\frac{\eta-\epsilon-\epsilon'-\omega_E}{\eta+\epsilon+\epsilon'+\omega_E}|(\frac{\delta}{(\epsilon+\epsilon'+\omega_E)^2+\delta^2} - \frac{\delta}{\eta^2+\delta^2}) + ln|\frac{\eta+\epsilon-\epsilon'-\omega_E}{\eta-\epsilon+\epsilon'+\omega_E}|(\frac{\delta}{(-\epsilon+\epsilon'+\omega_E)^2+\delta^2} - \frac{\delta}{\eta^2+\delta^2})) \quad \text{(B.18)}$$

In the case of $\delta \to 0$ the Einstein case is recovered.

APPENDIX C

An Alternative Derivation for The Electron Self-Energy

In this section, an alternative derivation for the self-energy will be given in the case of finite, frequency dependant density of states. This derivation is not intended to be used as a replacement to preceding derivations. The purpose of this derivation is to show that in case of an Einstein mode, and ultimately in the general case, the self-energy at a given frequency depends on frequencies at integer multiples of ω_E away from that frequency. The purpose of this exercise is to show that the restoration at $2\omega_E$ is expected because there is a minimum at ω_E.
New definitions are required before actual derivations are given:

$$n_0(\epsilon) = N_0(\epsilon) - N_0(\infty), \tag{C.1}$$

$$n(\epsilon) = N(\epsilon) - N(\infty), \tag{C.2}$$

$$\Sigma_0(\omega + i\delta) = \frac{\lambda\omega_E}{2} N(\infty) ln|\frac{\omega + i\delta - \omega_E}{\omega + i\delta + \omega_E}|. \tag{C.3}$$

At this point, it is important to note that, at infinity, the contribution from the finite band is not present. Therefore, the only contribution comes from the background band. Thus, it is safe to assume that:

$$N_0(\infty) = N(\infty). \tag{C.4}$$

Another point to be kept in mind in this derivation concerns the spectral function of electrons, which is defined as:

$$A(\epsilon, \omega) = -\frac{1}{\pi} ImG(\epsilon, \omega + i\delta), \tag{C.5}$$

and

$$ImG(\epsilon, \omega + i\delta) = -\frac{|Im\Sigma(\omega + i\delta)|}{(\omega - \epsilon - Re\Sigma(\omega + i\delta))^2 + Im\Sigma(\omega + i\delta)^2}. \tag{C.6}$$

The imaginary part of the self-energy is symmetric in frequency, and the real part is anti-symmetric. If one considers the function $ImG(-\epsilon, \omega + i\delta)$, one can write the above equation as:

$$ImG(-\epsilon, \omega + i\delta) = -\frac{|Im\Sigma(\omega + i\delta)|}{(\omega + \epsilon - Re\Sigma(\omega + i\delta))^2 + Im\Sigma(\omega + i\delta)^2} \tag{C.7}$$

or:

$$ImG(\epsilon, \omega + i\delta) = -\frac{|Im\Sigma(\omega + i\delta)|}{(-\omega - \epsilon + Re\Sigma(\omega + i\delta))^2 + Im\Sigma(\omega + i\delta)^2} \tag{C.8}$$

which is same as $ImG(\epsilon, -\omega + i\delta)$. Therefore:

$$ImG(-\epsilon, \omega + i\delta) = ImG(\epsilon, -\omega + i\delta). \tag{C.9}$$

From the relation of the Green function to the spectral function

$$A(-\epsilon, \omega) = A(\epsilon, -\omega) \tag{C.10}$$

Fortunately, the definition of the density of states is symmetric, so one can say, only for this case:

$$A(-\epsilon, \omega) = A(\epsilon, \omega). \tag{C.11}$$

As final preparation, the spectral representation of the Green function will be modified:

$$G(\epsilon, \omega + i\delta) = \int_{-\infty}^{\infty} d\omega' \frac{A(\epsilon, \omega')}{\omega + i\delta - \omega'} \tag{C.12}$$

or:

$$G(\epsilon, \omega + i\delta) = \int_{0}^{\infty} d\omega' \frac{A(\epsilon, \omega')}{\omega + i\delta - \omega'} + \int_{0}^{\infty} d\omega' \frac{A(\epsilon, -\omega')}{\omega + i\delta + \omega'}. \tag{C.13}$$

From equations B.5 and B.10, the self-energy is given by:

$$\Sigma(\omega+i\delta) = \frac{\lambda\omega_E}{2}\int_0^\infty d\epsilon' N(\epsilon')[\frac{1}{\omega+i\delta-\omega_E-\epsilon'}+\frac{1}{\omega+i\delta+\omega_E+\epsilon'}] \quad \text{(C.14)}$$

As done earlier, in order to isolate the singular portion, the constant piece will be added and subtracted.

$$\Sigma(\omega+i\delta) = \frac{\lambda\omega_E}{2}\{\int_0^\infty d\epsilon' n(\epsilon')[\frac{1}{\omega+i\delta-\omega_E-\epsilon'}+\frac{1}{\omega+i\delta+\omega_E+\epsilon'}] + N(\infty)ln|\frac{\omega+i\delta-\omega_E}{\omega+i\delta+\omega_E}|\} \quad \text{(C.15)}$$

The logarithmic part is $\Sigma_0(\omega+i\delta)$. In the integral, the definition of density of states is substituted:

$$\Sigma(\omega+i\delta) = \Sigma_0(\omega+i\delta) + \frac{\lambda\omega_E}{2}\int_0^\infty d\epsilon'(\int_{-\infty}^\infty d\xi n_0(\xi)A(\xi,\epsilon'))[\frac{1}{\omega+i\delta-\omega_E-\epsilon'}+\frac{1}{\omega+i\delta+\omega_E+\epsilon'}] \quad \text{(C.16)}$$

or:

$$\Sigma(\omega+i\delta) = \Sigma_0(\omega+i\delta)+\frac{\lambda\omega_E}{2}\int_{-\infty}^\infty d\xi n_0(\xi)\int_0^\infty d\epsilon'[\frac{A(\xi,\epsilon')}{\omega+i\delta-\omega_E-\epsilon'}+\frac{A(-\xi,\epsilon')}{\omega+i\delta+\omega_E+\epsilon'}]. \quad \text{(C.17)}$$

The first integral is that of the Green function with one component missing. So, integrals can be evaluated with proper arrangements:

$$\Sigma(\omega+i\delta) = \Sigma_0(\omega+i\delta) + \frac{\lambda\omega_E}{2}\int_{-\infty}^\infty d\xi n_0(\xi)\{G(\xi,\omega+\omega_E+i\delta)+G(\xi,\omega-\omega_E+i\delta) - \int_0^\infty d\epsilon'[\frac{A(-\xi,\epsilon')}{\omega+i\delta+\omega_E-\epsilon'}+\frac{A(\xi,\epsilon')}{\omega+i\delta-\omega_E+\epsilon'}]\} \quad \text{(C.18)}$$

or:

$$\Sigma(\omega+i\delta) = \Sigma_0(\omega+i\delta) + \frac{\lambda\omega_E}{2}\{\int_{-\infty}^\infty d\xi n_0(\xi)[G(\xi,\omega+\omega_E+i\delta)+G(\xi,\omega-\omega_E+i\delta)] - \int_0^\infty d\epsilon'[\frac{n(\epsilon')}{\omega+i\delta+\omega_E-\epsilon'}+\frac{n(\epsilon')}{\omega+i\delta-\omega_E+\epsilon'}]\} \quad \text{(C.19)}$$

The integral involving the Green function will be taken care of later. The second integral can be recognized as the self-energy itself. However, there is a slight modification. The arguments of the self-energy for the two parts are different. The proper result for these arguments is:

$$\Sigma(\omega+i\delta)=\Sigma_0(\omega+i\delta)+\frac{\lambda\omega_E}{2}\int_{-\infty}^{\infty}d\xi n_0(\xi)[G(\xi,\omega+\omega_E+i\delta)+G(\xi,\omega-\omega_E+i\delta)]$$
$$-\{\Sigma(\omega+2\omega_E+i\delta)+\Sigma(\omega-2\omega_E+i\delta)-\Sigma_0(\omega+2\omega_E+i\delta)-\Sigma_0(\omega+2\omega_E+i\delta)$$
$$-\frac{\lambda\omega_E}{2}\int_0^{\infty}d\epsilon'[\frac{n(\epsilon')}{\omega+i\delta+3\omega_E-\epsilon'}+\frac{n(\epsilon')}{\omega+i\delta-3\omega_E+\epsilon'}]\} \quad (C.20)$$

$\Sigma_0(\omega\pm 2\omega_E+i\delta)$ appears because the density of states given in the equation is the new defined one, involving a constant piece.

One can repeat the same procedure one more time, finding:

$$\Sigma(\omega+i\delta)=\Sigma_0(\omega+i\delta)+\frac{\lambda\omega_E}{2}\int_{-\infty}^{\infty}d\xi n_0(\xi)[G(\xi,\omega+\omega_E+i\delta)+G(\xi,\omega-\omega_E+i\delta)]$$
$$-\Sigma(\omega+2\omega_E+i\delta)-\Sigma(\omega-2\omega_E+i\delta)+\Sigma_0(\omega+2\omega_E+i\delta)+\Sigma_0(\omega+2\omega_E+i\delta)$$
$$+\frac{\lambda\omega_E}{2}[\int_{-\infty}^{\infty}d\xi n_0(\xi)[G(\xi,\omega+3\omega_E+i\delta)+G(\xi,\omega-3\omega_E+i\delta)]$$
$$-\Sigma(\omega+4\omega_E+i\delta)-\Sigma(\omega-4\omega_E+i\delta)+\Sigma_0(\omega+4\omega_E+i\delta)+\Sigma_0(\omega+4\omega_E+i\delta)$$
$$+\frac{\lambda\omega_E}{2}\int_0^{\infty}d\epsilon'[\frac{n(\epsilon')}{\omega+i\delta+5\omega_E-\epsilon'}+\frac{n(\epsilon')}{\omega+i\delta-5\omega_E+\epsilon'}])]\} \quad (C.21)$$

The procedure can be continued. At infinity, the contribution from the integral disappears, leaving the equation as:

$$\Sigma(\omega+i\delta)=\sum_{n=-\infty}^{\infty}\Sigma_0(\omega+n\omega_E+i\delta)+\frac{\lambda\omega_E}{2}\int_{-\infty}^{\infty}d\xi n_0(\xi)G(\xi,\omega+(2n-1)\omega_E+i\delta)-$$
$$(1-\delta_{n,0})\Sigma(\omega+2n\omega_E+i\delta) \quad (C.22)$$

The integral depends on the shape of the bare density of states. It can be evaluated analytically with contour integration, but it is not necessary for the purposes of this section. The equation relates the self-energy at a particular energy to that

at other, shifted energies. More importantly, it shows that the self-energy at a particular frequency is affected by features at other frequencies.

APPENDIX D

The Required Matsubara Summation

In this section, a standard Matsubara sum will be carried out[19]. The summation that needs to calculated is:

$$\frac{1}{\beta}\sum_n \frac{2\Omega}{\nu_n^2+\Omega^2}\frac{1}{i\omega_m - i\nu_n - \omega'} = \frac{-1}{\beta}\sum_n f(i\nu_n) \tag{D.1}$$

Consider the integral:

$$I = \lim_{R\to\infty}\oint \frac{dz}{2\pi i} f(z) n_B(z) \tag{D.2}$$

where

$$n_B(z) = \frac{1}{e^{\beta z}-1} \tag{D.3}$$

This function is chosen since as R goes to infinity, it has poles at the points $i2\pi n k_B T$ for all integers, n. The residue at those points is $1/\beta$. The function $f(z)$ has three poles. The poles and residues for those points are as follows.

$$\begin{aligned} z_n &= i2\pi n k_B T, & R_n &= \frac{1}{\beta} f(i\nu_n) \\ z_1 &= \Omega & R_1 &= \frac{n_B(\Omega)}{i\omega_m - i\omega' + \Omega} \\ z_2 &= -\Omega & R_2 &= \frac{n_B(\Omega)+1}{i\omega_m - i\omega' - \Omega} \\ z_3 &= \omega' - i\omega_m & R_3 &= \frac{-2\Omega n_F(\omega')}{(i\omega_m - \omega')^2 - \Omega^2} \end{aligned} \tag{D.4}$$

The last residue can be rewritten as:

$$R_3 = \frac{n_F(\omega')}{i\omega_m - \omega' + \Omega} - \frac{n_F(\omega')}{i\omega_m - \omega' - \Omega} \tag{D.5}$$

Therefore the total integral is:

$$I = \frac{1}{\beta}\sum_n f(i\nu_n) + \frac{n_B(\Omega) + n_F(\omega')}{i\omega_m - \omega' + \Omega} - \frac{n_B(\Omega) + 1 - n_F(\omega')}{i\omega_m - \omega' - \Omega} \tag{D.6}$$

As R approaches infinity, the integrands decay quickly to zero, and therefore the result of the integral is 0. Therefore:

$$-\frac{1}{\beta}\sum_n f(i\nu_n) = \frac{n_B(\Omega) + n_F(\omega')}{i\omega_m - \omega' + \Omega} - \frac{n_B(\Omega) + 1 - n_F(\omega')}{i\omega_m - \omega' - \Omega} \tag{D.7}$$

APPENDIX E

An Introduction to Green Functions

In this section, a standard textbook introduction and derivation for the method of Green functions will be given.[14] A similar derivation can be found in many condensed matter books.

For any Hamiltonian describing a particular system, the key point of the Green function methodology is the introduction of imaginary time, τ. Even though imaginary time itself is not practical, it can be converted to imaginary energy. Then, the function can be analytically continued to real energies. After that, possibly to real time.

The time evolution of an operator is given with respect to this imaginary time. Here the Heisenberg representation for electrons will be used. In the Heisenberg representation, the full time evolution is given to single particle operators:

$$c^{\dagger}_{k\sigma}(\tau) = U(\tau)c^{\dagger}_{k\sigma}U(-\tau) \tag{E.1}$$

where:

$$U(\tau) = exp(\tau\mathcal{H}) \tag{E.2}$$

where $\mathcal{H}$ is the system Hamiltonian. In this representation, the Green function is defined to be:

$$\mathcal{G}_{\sigma}(\mathbf{k};\tau-\tau') = -\langle T_{\tau}c_{k\sigma}(\tau)c^{\dagger}_{k\sigma}(\tau')\rangle. \tag{E.3}$$

The expectation value is:

$$\langle Q\rangle = tr\{Q\ exp[\beta(\Omega-\mathcal{H})]\} \tag{E.4}$$

where

$$exp(\beta\Omega) = tr\{exp(\beta\mathcal{H})\}. \tag{E.5}$$

The time ordering operator T_τ is defined to be:

$$T_\tau c(\tau)c^\dagger(\tau') = \begin{cases} c(\tau)c^\dagger(\tau'); \ (\tau > \tau') \\ -c^\dagger(\tau')c(\tau); \ (\tau < \tau') \end{cases}. \tag{E.6}$$

If $\tau > \tau'$, one electron is added at τ' and removed at τ. In this case the Green function describes the propagation of an electron from τ' to τ. If $\tau < \tau'$, one hole is added at τ' and removed at τ. In this case the Green function describes propagation of a hole from τ' to τ. One can also think of this case as propagation from τ to τ' of an electron.

Assuming $\mathcal{H}$ can be represented by orthonormal eigenfunctions $|\alpha\rangle$ with eigenvalues E_α, the functional form of the Green function can be written as:

$$\mathcal{G}(\mathbf{k}, \tau - \tau') = \sum_{\alpha\alpha'} |\langle\alpha'|c_\mathbf{k}^\dagger|\alpha\rangle|^2 exp[\beta(\Omega - E_\alpha)] exp[(E_{\alpha'} - E_\alpha)(\tau - \tau')] \\ \{-\theta(\tau - \tau') exp[\beta(E_\alpha - E_{\alpha'})] + \theta(\tau' - \tau)\}. \tag{E.7}$$

where $\theta(x)$ is the step function which appears due to time ordering operator. It is convenient to define the electron spectral function as:

$$A(\mathbf{k}, E) = f^{-1}(E) \sum_{\alpha\alpha'} |\langle\alpha'|c_\mathbf{k}^\dagger|\alpha\rangle|^2 exp[\beta(\Omega - E_\alpha)] \delta(E_\alpha - E_\alpha - E), \tag{E.8}$$

where $f(E)$ is the Fermi function. The spectral function is a non-negative function with normalized distribution. Therefore it can be considered as an energy (and momentum) probability distribution function for electrons. For the free electron case, the spectral function reduces to a delta function. With this definition, one can write the electron Green function as:

$$\mathcal{G}(\mathbf{k}, \tau) = \int_{-\infty}^{\infty} dE A(\mathbf{k}, E) exp[-E\tau]\{-\theta(\tau)[1 - f(E)] + \theta(-\tau) f(E)\}. \tag{E.9}$$

where $f(E)$ is the Fermi function for that temperature. Using the anti-periodicity of Green function, $\mathcal{G}(\mathbf{k}, \tau - \tau' + \beta) = -\mathcal{G}(\mathbf{k}, \tau - \tau')$, one can transform to energy space using the Fourier transformation:

$$\mathcal{G}(\mathbf{k}, \tau) = \beta^{-1} \sum_m \mathcal{G}(\mathbf{k}, i\omega_m) exp(-i\omega_m \tau) \tag{E.10}$$

where

$$\omega_m = \frac{2\pi}{\beta}(m + \frac{1}{2}), \ m = 0, \pm 1, \pm 2, \pm 3.... \tag{E.11}$$

The Green function in energy space can be written as:

$$\mathcal{G}(\mathbf{k}, i\omega_m) = \int_0^\beta d\tau \mathcal{G}(\mathbf{k}, \tau) exp(i\omega_m \tau). \tag{E.12}$$

Substituting the Green function in terms of spectral function results in:

$$\mathcal{G}(\mathbf{k}, i\omega_m) = \int_{-\infty}^{\infty} \frac{A(\mathbf{k}, E)}{i\omega_m - E} dE. \tag{E.13}$$

The spectral function does not depend on imaginary energies. Using analytic continuation, the result can be generalized to any frequency in the complex plane:

$$\mathcal{G}(\mathbf{k}, z) = \int_{-\infty}^{\infty} \frac{A(\mathbf{k}, E)}{z - E} dE. \tag{E.14}$$

The arguments given here can be generalized to phonon operators with modifications from fermions to bosons. Since phonons are bosons, one can use time reversal symmetry to show that the phonon spectral function is an odd function of energy. Therefore, the phonon version of equation E.14 can be rewritten as:

$$\mathcal{D}(\mathbf{k}, z) = \int_{-\infty}^{\infty} \frac{B(\mathbf{k}, E)}{z - E} dE, \tag{E.15}$$

$$\mathcal{D}(\mathbf{k}, z) = \int_0^{\infty} B(\mathbf{k}, E)(\frac{1}{z - E} - \frac{1}{z + E}) dE, \tag{E.16}$$

since:

$$B(\mathbf{k}, E) = -B(\mathbf{k}, -E) \tag{E.17}$$

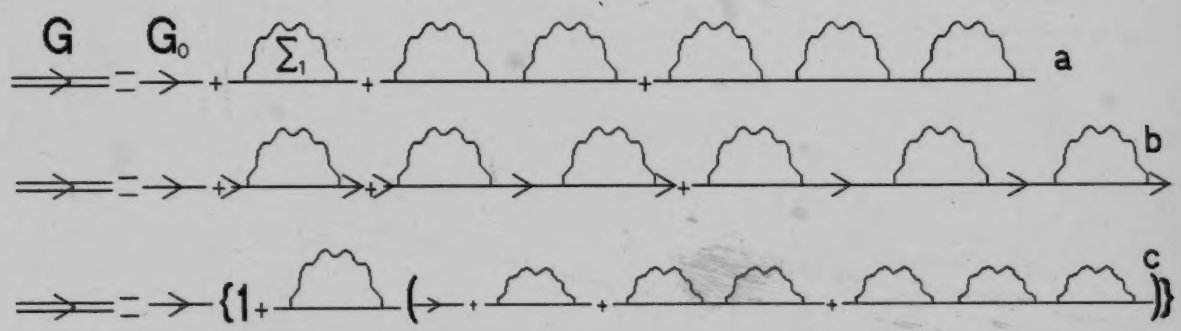

FIGURE E.1. Diagrammatic representation of full Green Function

E.1. Dyson Equation

The relation between the electron self-energy and the Green function is given by the Dyson equation. Here, a qualitative description for the origin of the Dyson equation will be given. The full Green function can be broken down into pieces according to the level of interaction between electrons and phonons. In general, the Green function contains any combination of interactions. Assuming that all these combinations are included in the electron self-energy, the equation can be reduced to:

$$\mathcal{G}(\mathbf{k}, i\omega_m) = \mathcal{G}_0(\mathbf{k}, i\omega_m) + \mathcal{G}_0(\mathbf{k}, i\omega_m)\Sigma(\mathbf{k}, i\omega_m)\mathcal{G}(\mathbf{k}, i\omega_m) \tag{E.18}$$

which can be modified to extract the full Green function as:

$$\mathcal{G}(\mathbf{k}, i\omega_m) = \frac{1}{\mathcal{G}_0^{-1}(\mathbf{k}, i\omega_m) - \Sigma(\mathbf{k}, i\omega_m)} \tag{E.19}$$

where $\mathcal{G}_0(\mathbf{k}, i\omega_m)$ is non-interacting Green function.

A schematic explanation of this equation for lowest order in self-energy, an electron interacting with a phonon, is given in Figure E.1. Fig.E.1a shows the full Green function with lowest order in self-energy. This form can be shown as in fig E.1b where the self-energy has been broken into irreducible pieces. First, each term

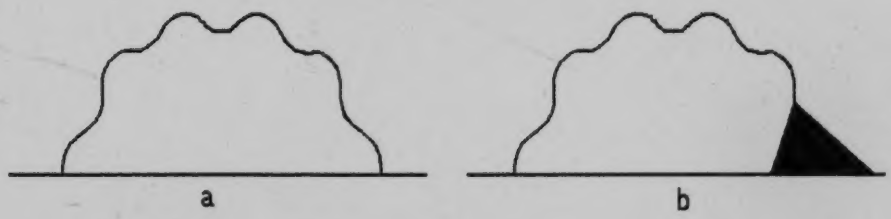

FIGURE E.2. Diagrammatic representation of electron self-energy

includes the non-interacting Green function, which can be taken out as a coefficient. Then, if one self-energy is taken out as a common factor from all terms involving the self-energy, the result becomes Figure E.1c. The part in parenthesis of the self-energy is identical to full Green function and can be replaced by it, resulting in:

$$\mathcal{G}(\mathbf{k}, i\omega_m) = \mathcal{G}_0(\mathbf{k}, i\omega_m) + \mathcal{G}_0(\mathbf{k}, i\omega_m)\Sigma_1(\mathbf{k}, i\omega_m)\mathcal{G}(\mathbf{k}, i\omega_m). \tag{E.20}$$

In this demonstration the lowest order approximation for the self-energy that can be used is shown in Figure E.2a. In general, self-energy can be written as this approximate function with a vertex correction which involves more complicated interactions as shown in Figure E.2b. If one replaces this correction into Figure E.1, the result becomes the Dyson equation.

APPENDIX F

The Electron Self-Energy With Angular Dependence

In this section, the derivation described in the Theory section will be carried out for angle dependant functions.

In this case, it is useful to separate the energy part and momentum parts of the q summation with a complete set of orthonormal functions, known as the Fermi surface harmonics:

$$\sum_k F_J(k)F_{J'}(k)\delta(\epsilon_k - \epsilon) = \delta_{J,J'}N(\epsilon), \tag{F.1}$$

where:

$$N(\epsilon) = \sum_k \delta(\epsilon_k - \epsilon). \tag{F.2}$$

The equations involved in this derivation can be rewritten in terms of the Fermi surface harmonics as:

$$\Sigma(k, i\omega_m) = \sum_J \Sigma_J(\epsilon_k, i\omega_m)F_J(k) \tag{F.3}$$

$$G(k, i\omega_m) = \sum_J G_J(\epsilon_k, i\omega_m)F_J(k) \tag{F.4}$$

$$\alpha^2F(k, k', \Omega) = \sum_{JJ'} \alpha^2F(JJ', \epsilon_k, \epsilon_{k'}, \Omega)F_J(k)F_{J'}(k'). \tag{F.5}$$

Substituting these forms in equation 2.8,

$$\Sigma(k, i\omega_m) = \frac{1}{\beta}\sum_{k',nJ,J'J''}\int_0^\infty d\Omega \frac{\alpha^2F(JJ', \epsilon_k, \epsilon_{k'}, \Omega)F_J(k)F_{J'}(k')}{N(0)}\frac{2\Omega}{\nu_n^2 + \Omega^2}$$
$$G_{J''}(\epsilon_{k'}, i\omega_m - i\nu_n)F_{J''}(k'). \tag{F.6}$$

Using the orthonormality between J' and J":

$$\Sigma(k,i\omega_m)=\frac{1}{\beta}\sum_{n,J,J'}\int_{-\infty}^{\infty}d\epsilon\frac{N(\epsilon)}{N(0)}\int_0^{\infty}d\Omega\alpha^2F(JJ',\epsilon_k,\epsilon,\Omega)F_J(k)\frac{2\Omega}{\nu_n^2+\Omega^2}$$
$$G_{J'}(\epsilon,i\omega_m-i\nu_n). \quad \text{(F.7)}$$

Rearranging gives:

$$\Sigma(k,i\omega_m)=\sum_J\{\frac{-1}{\beta}\sum_{n,J'}\int_{-\infty}^{\infty}d\epsilon\frac{N(\epsilon)}{N(0)}\int_0^{\infty}d\Omega\alpha^2F(JJ',\epsilon_k,\epsilon,\Omega)\frac{2\Omega}{\nu_n^2+\Omega^2}$$
$$G_{J'}(\epsilon,i\omega_m-i\nu_n)\}F_J(k). \quad \text{(F.8)}$$

The portion in curly brackets is corresponding to $\Sigma_J(\epsilon_k,i\omega_m)$.

$$\Sigma_J(k,i\omega_m)=\frac{1}{\beta}\sum_{n,J'}\int_{-\infty}^{\infty}d\epsilon\frac{N(\epsilon)}{N(0)}\int_0^{\infty}d\Omega\alpha^2F(JJ',k,\Omega)\frac{2\Omega}{\nu_n^2+\Omega^2}G_{J'}(\epsilon,i\omega_m-i\nu_n). \quad \text{(F.9)}$$

Thermodynamical properties of electrons can be described by this equation. However, for complete dynamical properties, an analytic continuation to the real axis is required. Before changing the arguments, all Matsubara sums on the right hand side should be calculated. Otherwise the continuation is not correct. To separate Matsubara sum from other functions, the spectral representation for the electron Green function will be used:

$$G(\epsilon,\omega+i\delta)=\int_{-\infty}^{\infty}d\omega'\frac{A(\epsilon,\omega')}{\omega+i\delta-\omega'}, \quad \text{(F.10)}$$

leading to:

$$\Sigma_J(k,i\omega_m)=\frac{1}{\beta}\sum_{n,J'}\int_{-\infty}^{\infty}d\epsilon\frac{N(\epsilon)}{N(0)}\int_0^{\infty}d\Omega\alpha^2F(JJ',k,\Omega)\frac{2\Omega}{\nu_n^2+\Omega^2}$$
$$\int_{-\infty}^{\infty}d\omega'\frac{A_{J'}(\epsilon,\omega')}{i\omega_m-i\nu_n-\omega'}. \quad \text{(F.11)}$$

Separating Matsubara sum as:

$$I(i\omega_m, \Omega, \omega') = \frac{1}{\beta}\sum_n \frac{2\Omega}{\nu_n^2 + \Omega^2}\frac{1}{i\omega_m - i\nu_n - \omega'}, \tag{F.12}$$

as shown in Appendix D, this sum is equal to:

$$I(i\omega_m, \Omega, \omega') = \frac{n(\Omega) + f(-\omega')}{i\omega - \Omega - \omega'} + \frac{n(\Omega) + f(\omega')}{i\omega + \Omega - \omega'} \tag{F.13}$$

Since the index J defines a complete orthogonal set, any off-diagonal term is zero. Using this property;

$$\sum_J \alpha^2 F(JJ', k, \Omega) F_J(k) = \sum_{k'} \frac{\alpha^2 F(kk', \Omega)}{N(0)} \equiv \alpha^2 F(k, \Omega) \tag{F.14}$$

With these new definitions, the self-energy can be written as:

$$\Sigma(k, i\omega_m) = \sum_{J'} \int_{-\infty}^{\infty} d\epsilon \frac{N(\epsilon)}{N(0)} \int_0^{\infty} d\Omega \alpha^2 F(k, \Omega) \int_{-\infty}^{\infty} d\omega' A_{J'}(\epsilon, \omega') I(i\omega_m, \Omega, \omega') \tag{F.15}$$

Normally, $\alpha^2 F(k, \Omega)$ is directly taken from experiments. Since that function involves the phonon spectral function, all phonon properties concerning electron-phonon interactions are measured and included as input from experiments. Therefore no separate derivation for phonons is required.

At this point, the imaginary axis frequencies can be analytically continued to any frequency on the upper complex plane($i\omega_m \rightarrow z$).

$$\Sigma(k, z) = \sum_{J'} \int_{-\infty}^{\infty} d\epsilon \frac{N(\epsilon)}{N(0)} \int_0^{\infty} d\Omega \alpha^2 F(k, \Omega) \int_{-\infty}^{\infty} d\omega' A_{J'}(\epsilon, \omega') I(z, \Omega, \omega') \tag{F.16}$$

If all angular dependencies are removed, this equation can be reduced to equation 2.17.